NLO QCD corrections to WW+jet production including leptonic W decays at hadron colliders

Stefan Kallweit[1]

in collaboration with S. Dittmaier and P. Uwer

based on Phys. Rev. Lett. **100**, 062003 (2008), PhD thesis of S.K.,
arXiv:0908.4124 [hep-ph] (to appear in Nucl. Phys. B)

[1]Paul Scherrer Institut, Würenlingen und Villigen

October 26, Radcor 2009

Outline

Relevance of $pp/p\bar{p} \to WW + \text{jet} + X$

- Important background process at the LHC (and for Tevatron Higgs searches):
  - background to Higgs searches: $H + \text{jet}$,
  - background to new-physics searches: $\text{leptons} + \not{E}_T + \text{jet}$.

$\hookrightarrow$ $VV + \text{jet}$ is on the top of the "Les Houches experimenter's wishlist '05"

Progress on $VV + \text{jet}$ so far:

- $pp \to WW + \text{jet}$ — Dittmaier/S.K./Uwer '07, '09; Campbell/Ellis/Zanderighi '07; Binoth/Guillet/Karg/Kauer/Sanguinetti (in progress)
- $pp \to W\gamma + \text{jet}$ — Campanario/Englert/Spannowsky/Zeppenfeld '09

Relevance of $\mathrm{pp}/\mathrm{p\bar{p}} \to \mathrm{WW} + \mathrm{jet} + \mathrm{X}$

- Important background process at the LHC (and for Tevatron Higgs searches):
  - background to Higgs searches: $\mathrm{H} + \mathrm{jet}$,
  - background to new-physics searches: $\mathrm{leptons} + \not{E}_{\mathrm{T}} + \mathrm{jet}$.

  $\hookrightarrow$ $\mathrm{VV} + \mathrm{jet}$ is on the top of the "Les Houches experimenter's wishlist '05"

  Progress on $\mathrm{VV} + \mathrm{jet}$ so far:
  - $\mathrm{pp} \to \mathrm{WW} + \mathrm{jet}$ — Dittmaier/S.K./Uwer '07, '09; Campbell/Ellis/Zanderighi '07; Binoth/Guillet/Karg/Kauer/Sanguinetti (in progress)
  - $\mathrm{pp} \to \mathrm{W}\gamma + \mathrm{jet}$ — Campanario/Englert/Spannowsky/Zeppenfeld '09
- A large fraction of W-pair events at the LHC show additional jet activity.
  $\hookrightarrow$ EW gauge-boson coupling analysis

Relevance of $pp/p\bar{p} \to WW + \text{jet} + X$

- Important background process at the LHC (and for Tevatron Higgs searches):
  - background to Higgs searches: $H + \text{jet}$,
  - background to new-physics searches: $\text{leptons} + \not{E}_T + \text{jet}$.

  $\hookrightarrow$ $VV + \text{jet}$ is on the top of the "Les Houches experimenter's wishlist '05"

  Progress on $VV + \text{jet}$ so far:
  - $pp \to WW + \text{jet}$ — Dittmaier/S.K./Uwer '07, '09; Campbell/Ellis/Zanderighi '07; Binoth/Guillet/Karg/Kauer/Sanguinetti (in progress)
  - $pp \to W\gamma + \text{jet}$ — Campanario/Englert/Spannowsky/Zeppenfeld '09
- A large fraction of W-pair events at the LHC show additional jet activity.
  $\hookrightarrow$ EW gauge-boson coupling analysis
- WW+jet delivers the real–virtual contribution to WW production at NNLO QCD.
  (two-loop results known [Chachamis, Czakon, Eiras '08])

Relevance of $pp/p\bar{p} \to WW + \text{jet} + X$

- Important background process at the LHC (and for Tevatron Higgs searches):
  - background to Higgs searches: $H + \text{jet}$,
  - background to new-physics searches: $\text{leptons} + \not{E}_T + \text{jet}$.

  $\hookrightarrow$ $VV + \text{jet}$ is on the top of the "Les Houches experimenter's wishlist '05"

  Progress on $VV + \text{jet}$ so far:
  - $pp \to WW + \text{jet}$ — Dittmaier/S.K./Uwer '07, '09; Campbell/Ellis/Zanderighi '07; Binoth/Guillet/Karg/Kauer/Sanguinetti (in progress)
  - $pp \to W\gamma + \text{jet}$ — Campanario/Englert/Spannowsky/Zeppenfeld '09
- A large fraction of W-pair events at the LHC show additional jet activity.
  $\hookrightarrow$ EW gauge-boson coupling analysis
- WW+jet delivers the real–virtual contribution to WW production at NNLO QCD. (two-loop results known [Chachamis, Czakon, Eiras '08])
- Process was an important test ground before approaching more complicated many-particle processes at NLO.

Hadronic cross section

Schematic illustration of the hadronic process $\mathrm{pp}/\mathrm{p\bar{p}} \to \mathrm{W^+W^-} + \mathrm{jet} + \mathrm{X}$:

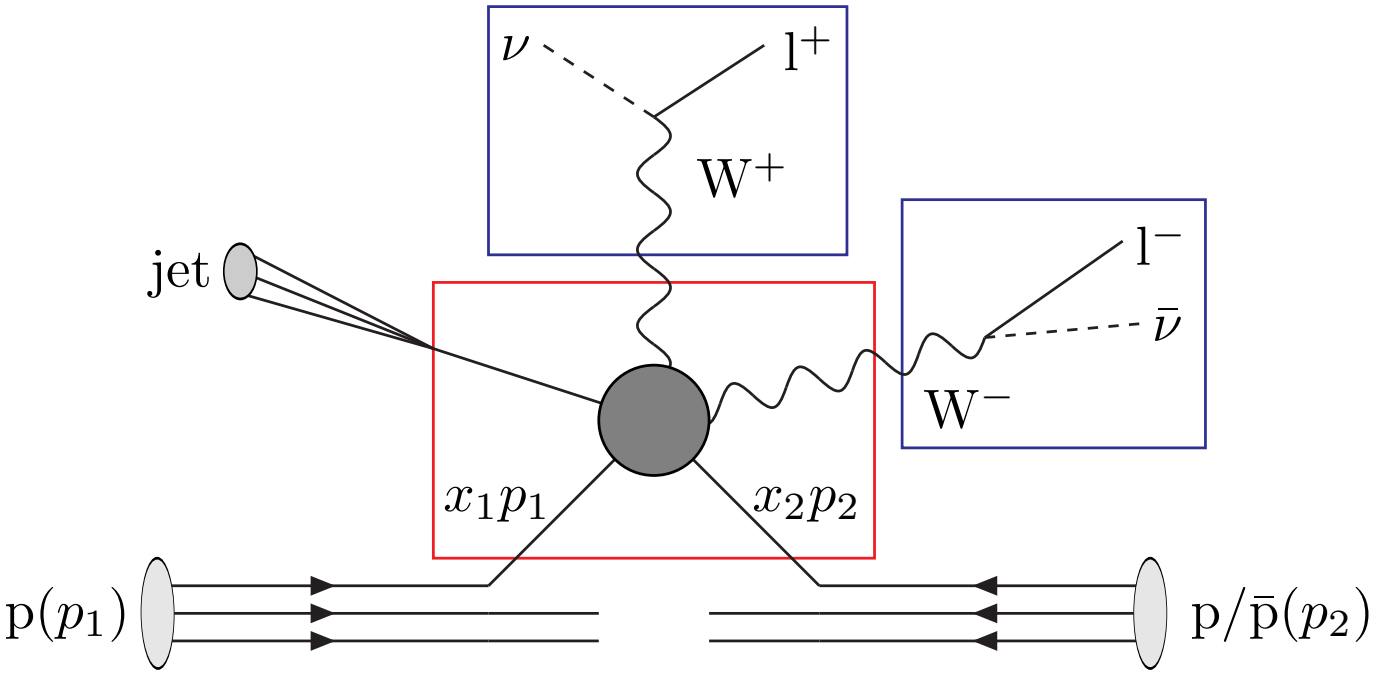

$$\sigma^{\mathrm{pp}/\mathrm{p\bar{p}}}(p_1, p_2) = \sum_{a,b} \int_0^1 dx_1 \int_0^1 dx_2 \underbrace{f_{a(\mathrm{p})}(x_1, \mu_\mathrm{F})\, f_{b(\mathrm{p}/\bar{\mathrm{p}})}(x_2, \mu_\mathrm{F})}_{\text{PDF's of parton } a/b \text{ in } \mathrm{p}/\bar{\mathrm{p}}} \underbrace{\hat{\sigma}^{ab}(x_1 p_1, x_2 p_2)}_{\text{partonic cross section}}$$

Subprocesses contributing at leading order

6 partonic channels in LO (12 flavour channels for 2 generations, b quarks omitted):

$$u\bar{u} \to W^+W^-g, \quad ug \to W^+W^-u, \quad g\bar{u} \to W^+W^-\bar{u},$$
$$d\bar{d} \to W^+W^-g, \quad dg \to W^+W^-d, \quad g\bar{d} \to W^+W^-\bar{d}$$

Diagrams for $u\bar{u}$ initial state:

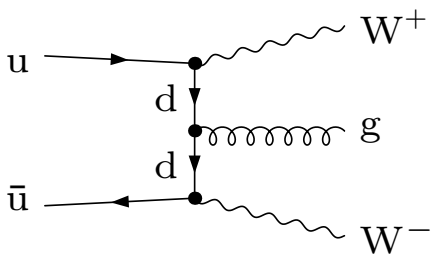

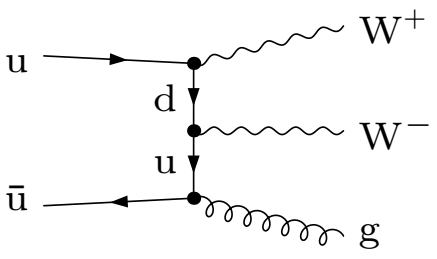

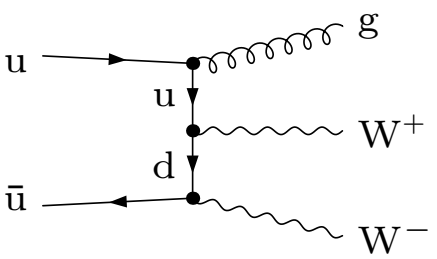

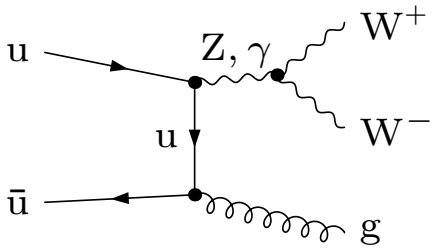

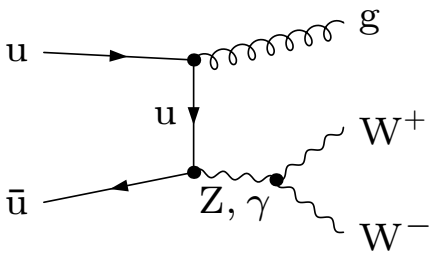

- all light quarks massless
- CKM matrix → Cabibbo matrix

↪ no CKM dependence in LO (unitarity)

Subprocesses contributing at leading order

6 partonic channels in LO (12 flavour channels for 2 generations, b quarks omitted):

$$\mathrm{u\bar{u}} \to \mathrm{W^+W^-g}, \quad \mathrm{ug} \to \mathrm{W^+W^-u}, \quad \mathrm{g\bar{u}} \to \mathrm{W^+W^-\bar{u}},$$
$$\mathrm{d\bar{d}} \to \mathrm{W^+W^-g}, \quad \mathrm{dg} \to \mathrm{W^+W^-d}, \quad \mathrm{g\bar{d}} \to \mathrm{W^+W^-\bar{d}}$$

Diagrams for $\mathrm{u\bar{u}}$ initial state:

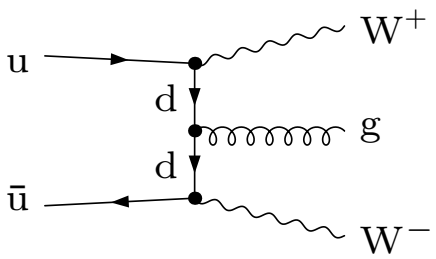

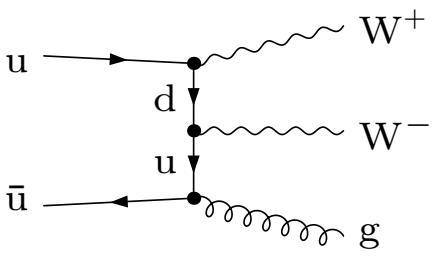

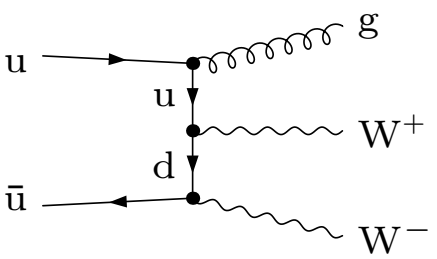

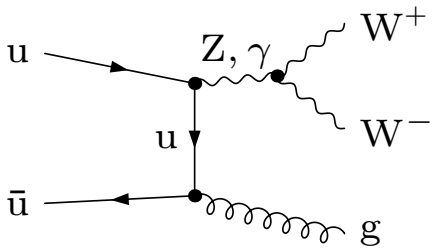

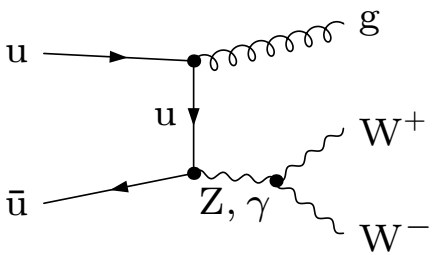

- all light quarks massless
- CKM matrix → Cabibbo matrix

↪ no CKM dependence in LO (unitarity)

The amplitudes for all other channels are generated by crossing the gluon into the initial state and by SU(2) symmetry ($\mathrm{u} \leftrightarrow \mathrm{d}, \mathrm{W^+} \leftrightarrow \mathrm{W^-}$).

Leading-order prediction

Scale dependence of LO cross section (with $\mu = \mu_{\text{fact}} = \mu_{\text{ren}}$):

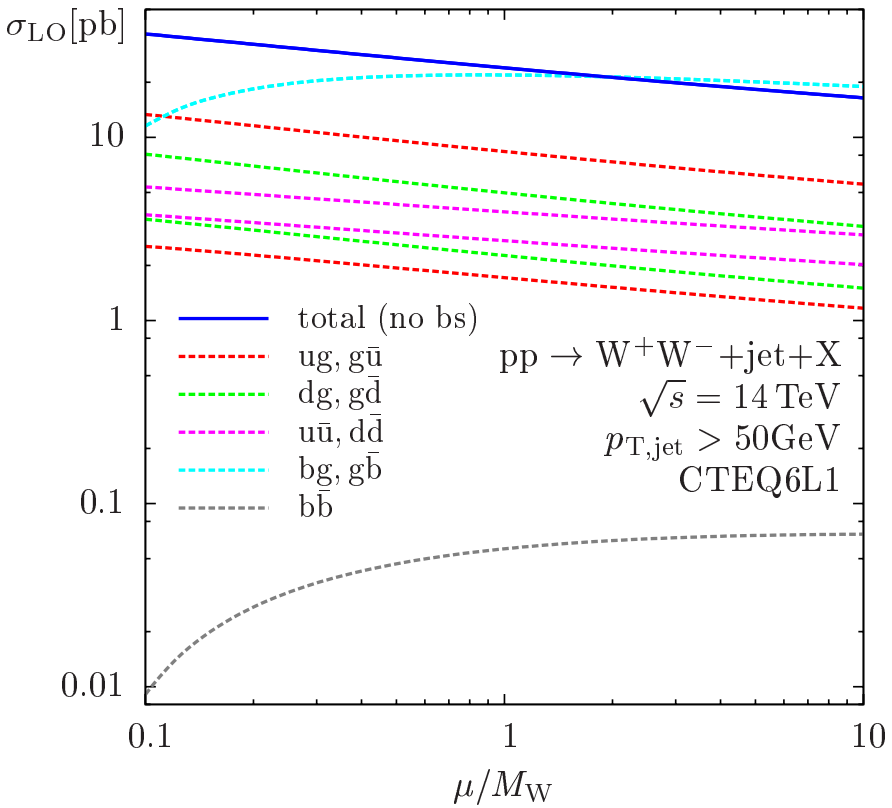

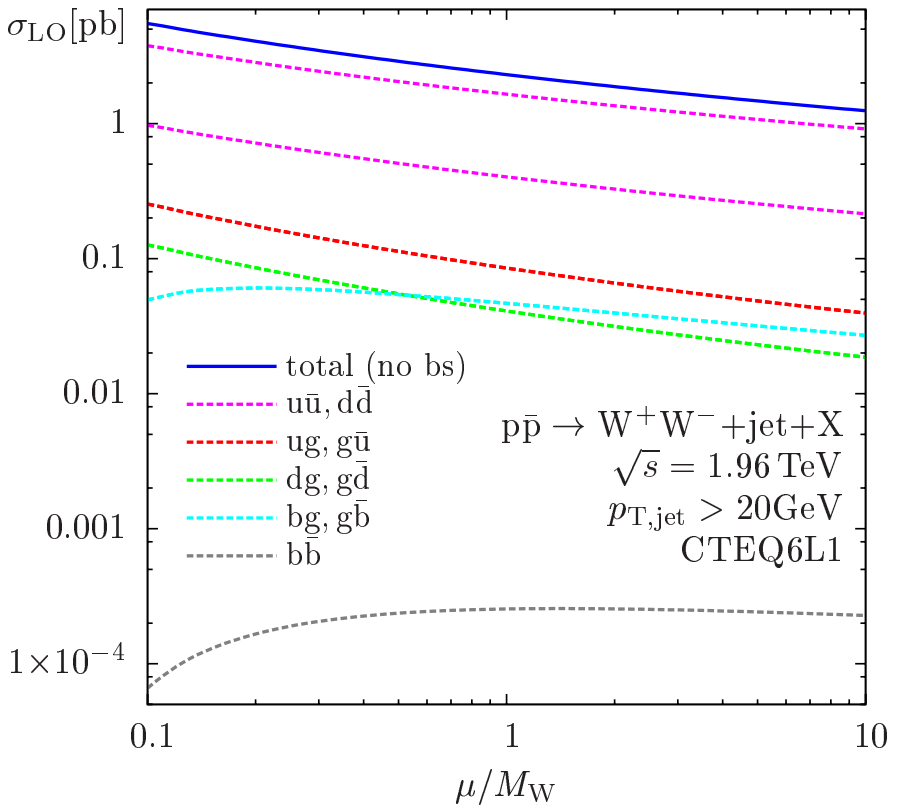

LHC: Cross section changes by 12% (30%) when scaling μ by a factor of 2 (5).
Tevatron: Cross section changes by 25% (75%) when scaling μ by a factor of 2 (5).

$\hookrightarrow$ For precise predictions the calculation of NLO QCD corrections is required.

NLO cross section with the dipole subtraction formalism

Schematic formula for the NLO cross section in the situation of two initial-state hadrons (LHC and Tevatron):

$$\sigma^{\mathrm{NLO}} = \underbrace{\int_{m+1} d\sigma^R}_{\text{real corrections}} + \underbrace{\int_m d\sigma^V}_{\text{virtual corrections}} + \underbrace{\int_0^1 dx \int_m d\sigma^C}_{\text{collinear-subtraction counterterm}}$$

NLO cross section with the dipole subtraction formalism

Schematic formula for the NLO cross section in the situation of two initial-state hadrons (LHC and Tevatron):

$$\sigma^{\mathrm{NLO}} = \underbrace{\int_{m+1} d\sigma^R}_{\text{real corrections}} + \underbrace{\int_m d\sigma^V}_{\text{virtual corrections}} + \underbrace{\int_0^1 dx \int_m d\sigma^C}_{\text{collinear-subtraction counterterm}} - \int_{m+1} d\sigma^A + \int_{m+1} d\sigma^A,$$

$$d\sigma^A = \sum_{\text{dipoles}} d\sigma^B \otimes dV_{\text{dipole}}$$

NLO cross section with the dipole subtraction formalism

Schematic formula for the NLO cross section in the situation of two initial-state hadrons (LHC and Tevatron):

$$\sigma^{\mathrm{NLO}} = \underbrace{\int_{m+1} d\sigma^R}_{\text{real corrections}} + \underbrace{\int_m d\sigma^V}_{\text{virtual corrections}} + \underbrace{\int_0^1 dx \int_m d\sigma^C}_{\text{collinear-subtraction counterterm}} - \int_{m+1} d\sigma^A + \int_{m+1} d\sigma^A,$$

$$d\sigma^A = \sum_{\text{dipoles}} d\sigma^B \otimes dV_{\text{dipole}}$$

$$= \int_{m+1} \left[d\sigma^R - d\sigma^A \right]_{\epsilon=0} \qquad \Rightarrow \mathrm{R} - \mathrm{A}$$

$$+ \int_m \left[d\sigma^V + \sum_{\text{dipoles}} d\sigma^B \otimes V_{\text{dipole}}(1) \right]_{\epsilon=0} \qquad \Rightarrow \mathrm{V} + \mathrm{A}$$

$$+ \int_0^1 dx \int_m \left[d\sigma^C + \sum_{\text{dipoles}} \int_1 d\sigma^B(x) \otimes \left[dV_{\text{dipole}}(x) \right]_+ \right]_{\epsilon=0} \qquad \Rightarrow \mathrm{C} + \mathrm{A}$$

$$dV_{\text{dipole}}(x) = \left[dV_{\text{dipole}}(x) \right]_+ + dV_{\text{dipole}}(1)\delta(1-x)$$

Virtual corrections

For each channel $\mathcal{O}(100)$ 1-loop diagrams contribute, which can be classified as

- "bosonic" corrections (exchange of an additional gluon)
- "fermionic" corrections (closed quark loops)

Renormalization leads to counterterm diagrams contributing on 1-loop level.

Virtual corrections

For each channel $\mathcal{O}(100)$ 1-loop diagrams contribute, which can be classified as

- "bosonic" corrections (exchange of an additional gluon)
- "fermionic" corrections (closed quark loops)

Renormalization leads to counterterm diagrams contributing on 1-loop level.

- Bosonic corrections: e. g. pentagon contributions (5-point functions)

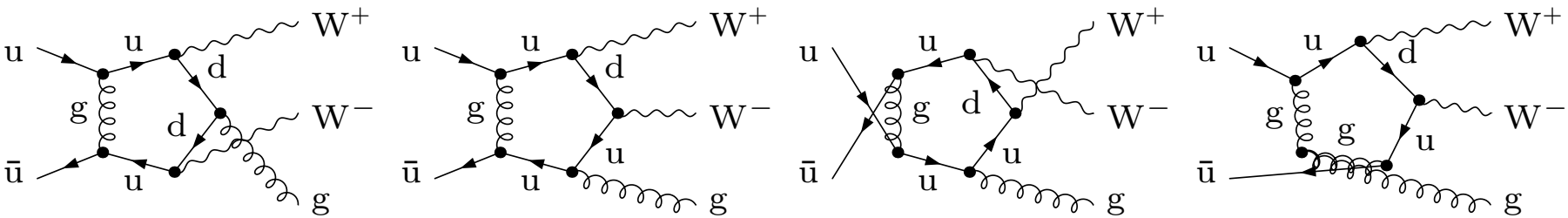

Virtual corrections

For each channel $\mathcal{O}(100)$ 1-loop diagrams contribute, which can be classified as

- "bosonic" corrections (exchange of an additional gluon)
- "fermionic" corrections (closed quark loops)

Renormalization leads to counterterm diagrams contributing on 1-loop level.

- Bosonic corrections: e. g. pentagon contributions (5-point functions)

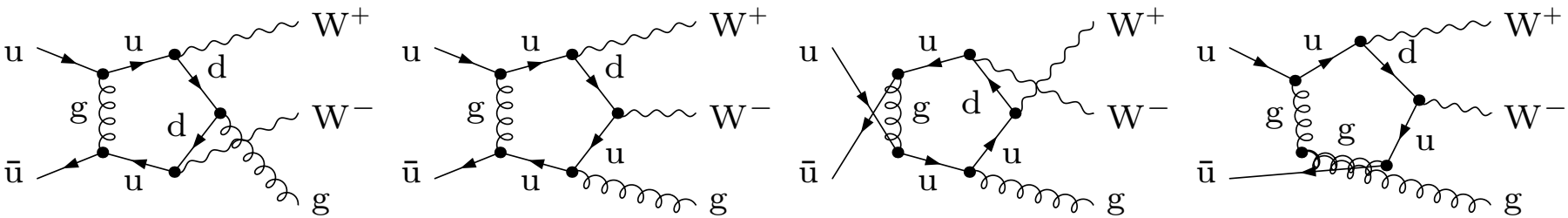

- Fermionic corrections: e. g. box contributions (4-point functions)

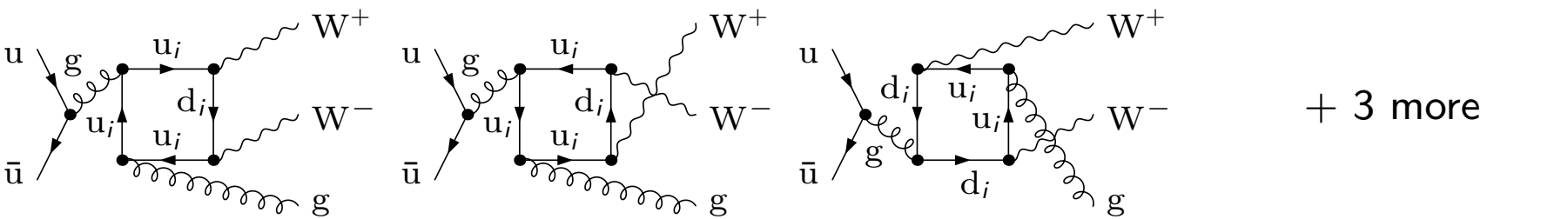

+ 3 more

Virtual corrections

Two different strategies for evaluation of loop amplitudes
(realized in two independent calculations!)

- Analogous to NLO calculation for
  $pp \to t\bar{t}H$ [Beenakker et al. '02] and $pp \to t\bar{t} + jet$ [Dittmaier, Uwer, Weinzierl '07]
  - diagrams generated with FeynArts 1.0 [Küblbeck, Böhm, Denner '90] and reduced with in-house Mathematica routines $\to$ Fortran
  - analytical extraction of IR singularities [Beenakker et al. '02, Dittmaier '03]
  - reduction of 5-point to 4-point integrals according to [Denner, Dittmaier '02], numerical stabilization for exceptional momentum regions via expansions [DD '05]

Virtual corrections

Two different strategies for evaluation of loop amplitudes
(realized in two independent calculations!)

- Analogous to NLO calculation for
  $pp \to t\bar{t}H$ [Beenakker et al. '02] and $pp \to t\bar{t} + jet$ [Dittmaier, Uwer, Weinzierl '07]
  - diagrams generated with FeynArts 1.0 [Küblbeck, Böhm, Denner '90] and reduced with in-house Mathematica routines → Fortran
  - analytical extraction of IR singularities [Beenakker et al. '02, Dittmaier '03]
  - reduction of 5-point to 4-point integrals according to [Denner, Dittmaier '02], numerical stabilization for exceptional momentum regions via expansions [DD '05]
- Alternative calculation with available tools
  - diagrams generated with FeynArts 3.4 [Hahn '00]
  - algebraic reduction/numerical evaluation with FormCalc 6.0/LoopTools: [Hahn, Perez-Victoria '98]
    - reduction of 5-point integrals à la [Denner, Dittmaier '02]
    - regular scalar integrals with FF [v.Oldenborgh '91]
  - dimensionally regularized singular integrals added to LoopTools:
    - box integrals checked against result of [Bern, Dixon, Kosower '93]

Real corrections

Contributing subprocesses are generated by two types of generic amplitudes,

- $0 \to \mathrm{W}^+\mathrm{W}^-\mathrm{q}\bar{\mathrm{q}}\mathrm{g}\mathrm{g}$,
- $0 \to \mathrm{W}^+\mathrm{W}^-\mathrm{q}\bar{\mathrm{q}}\mathrm{q}'\bar{\mathrm{q}}'$,

and crossing any two partons into the initial state.
$\hookrightarrow$ Large number of contributions (136 flavour channels for 2 generations)!

Sample of real-correction diagrams:

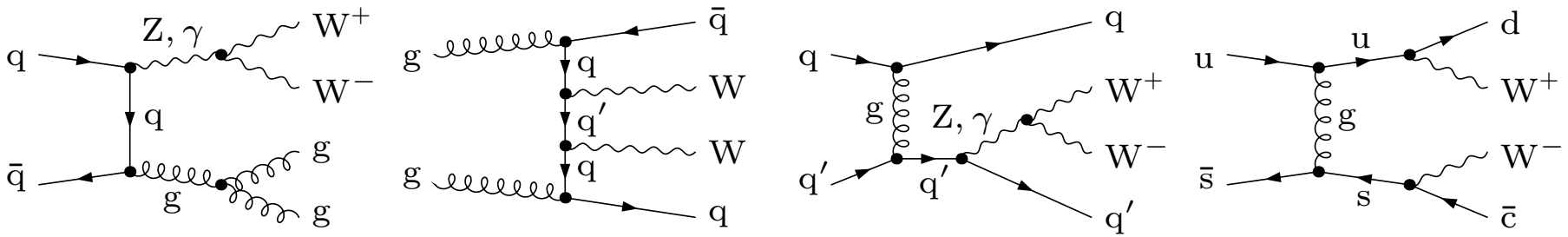

Real corrections

Contributing subprocesses are generated by two types of generic amplitudes,

- $0 \to \mathrm{W}^+\mathrm{W}^-\mathrm{q}\bar{\mathrm{q}}\mathrm{g}\mathrm{g}$,
- $0 \to \mathrm{W}^+\mathrm{W}^-\mathrm{q}\bar{\mathrm{q}}\mathrm{q}'\bar{\mathrm{q}}'$,

and crossing any two partons into the initial state.
$\hookrightarrow$ Large number of contributions (136 flavour channels for 2 generations)!

Sample of real-correction diagrams:

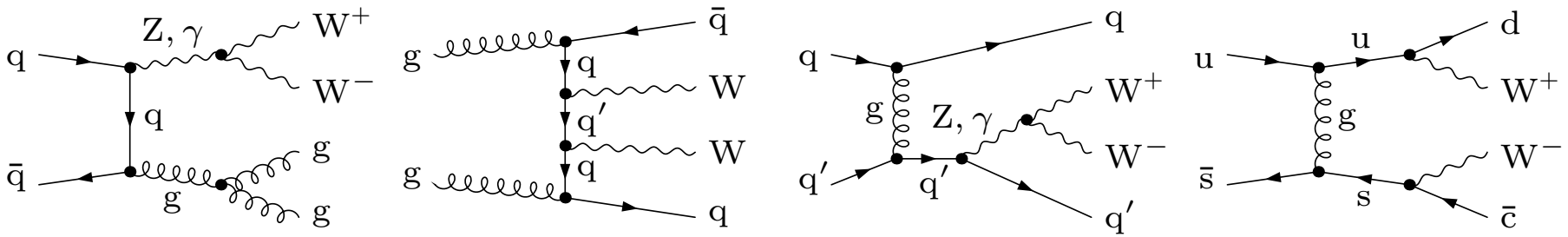

Two evaluations of helicity amplitudes:

- application of (4-dimensional) spinor techniques
- alternative evaluation based on MADGRAPH [Stelzer, Long '94]

Real corrections

Contributing subprocesses are generated by two types of generic amplitudes,

- $0 \to \mathrm{W}^+\mathrm{W}^-\mathrm{q}\bar{\mathrm{q}}\mathrm{g}\mathrm{g}$,
- $0 \to \mathrm{W}^+\mathrm{W}^-\mathrm{q}\bar{\mathrm{q}}\mathrm{q}'\bar{\mathrm{q}}'$,

and crossing any two partons into the initial state.
↪ Large number of contributions (136 flavour channels for 2 generations)!

Sample of real-correction diagrams:

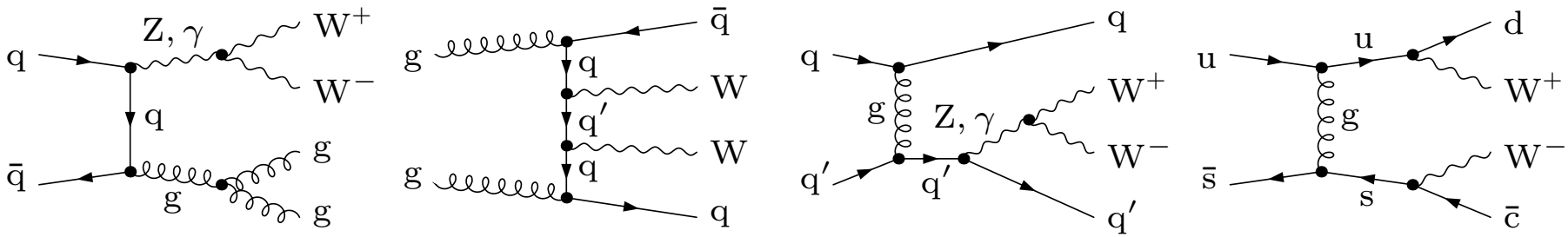

Two evaluations of helicity amplitudes:

- application of (4-dimensional) spinor techniques
- alternative evaluation based on MADGRAPH [Stelzer, Long '94]

Two versions of Monte Carlo integrators:

- based on multi-channel MC technique [Berends, Pittau, Kleis '94, Kleis, Pittau '94]
- second version based on simple mapping (phase space by sequential splitting)

W decays via improved NWA

Double-resonant diagrams:

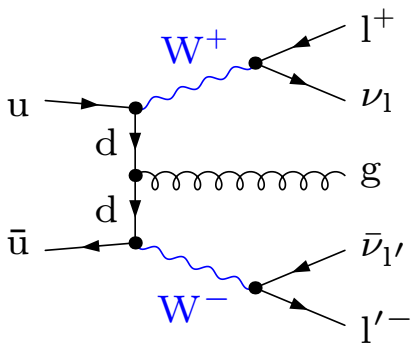

$k^2_{\mathrm{W}} \longrightarrow M^2_{\mathrm{W}}$

Single-resonant diagrams:

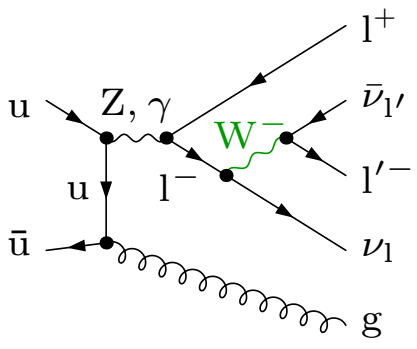

neglected!

W decays via improved NWA

Double-resonant diagrams:

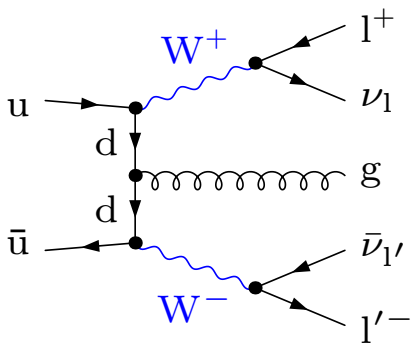

$k_W^2 \longrightarrow M_W^2$

Single-resonant diagrams:

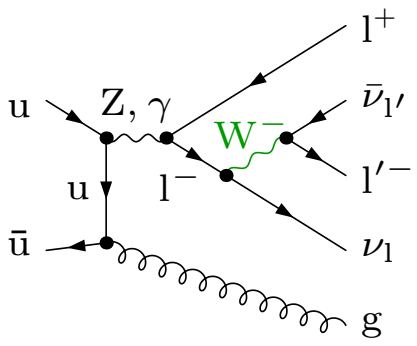

neglected!

- on-shell approximation for resonant matrix elements:

$$\mathcal{M}_{\text{resonant}} \sim \sum_{\lambda_W} \frac{\mathcal{M}^W_{\text{prod}}(k_W^2 \longrightarrow M_W^2, \lambda_W) \times \mathcal{M}^W_{\text{decay}}(k_W^2 \longrightarrow M_W^2, \lambda_W)}{k_W^2 - M_W^2 + i\Gamma_W M_W}$$

Spin correlations respected!

W decays via improved NWA

Double-resonant diagrams:

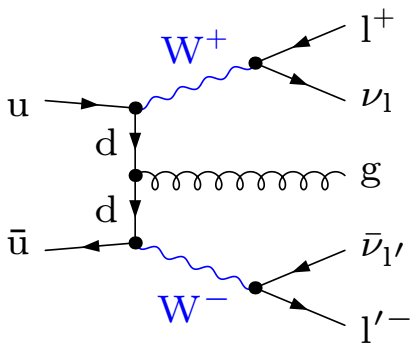

$k_{\mathrm{W}}^2 \longrightarrow M_{\mathrm{W}}^2$

Single-resonant diagrams:

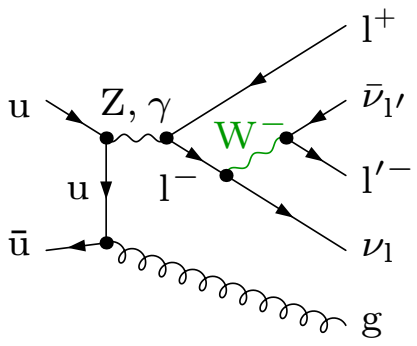

neglected!

- on-shell approximation for resonant matrix elements:

$$\mathcal{M}_{\mathrm{resonant}} \sim \sum_{\lambda_{\mathrm{W}}} \frac{\mathcal{M}^{\mathrm{W}}_{\mathrm{prod}}(k_{\mathrm{W}}^2 \longrightarrow M_{\mathrm{W}}^2, \lambda_{\mathrm{W}}) \times \mathcal{M}^{\mathrm{W}}_{\mathrm{decay}}(k_{\mathrm{W}}^2 \longrightarrow M_{\mathrm{W}}^2, \lambda_{\mathrm{W}})}{k_{\mathrm{W}}^2 - M_{\mathrm{W}}^2 + \mathrm{i}\Gamma_{\mathrm{W}} M_{\mathrm{W}}}$$

Spin correlations respected!

- replacement of Breit–Wigner-propagator by a δ-function approximation:

$$\int_{\mathrm{min}}^{\mathrm{max}} dk_{\mathrm{W}}^2 \int d\Phi^{\mathrm{W}}_{\mathrm{prod}}(k_{\mathrm{W}}^2) \frac{1}{(k_{\mathrm{W}}^2 - M_{\mathrm{W}}^2)^2 + \Gamma_{\mathrm{W}}^2 M_{\mathrm{W}}^2} \int d\Phi^{\mathrm{W}}_{\mathrm{decay}}(k_{\mathrm{W}}^2)$$

$$\longrightarrow \int_{-\infty}^{\infty} dk_{\mathrm{W}}^2 \int d\Phi^{\mathrm{W}}_{\mathrm{prod}}(M_{\mathrm{W}}^2) \frac{\pi}{\Gamma_{\mathrm{W}} M_{\mathrm{W}}} \delta(k_{\mathrm{W}}^2 - M_{\mathrm{W}}^2) \int d\Phi^{\mathrm{W}}_{\mathrm{decay}}(M_{\mathrm{W}}^2)$$

W decays via improved NWA

Two different (equivalent) implementation strategies

$\hat{k} = \hat{k}_1 + \hat{k}_2, \ \hat{k}^2 = M_V^2$

- Decay correlation matrix

$$\sigma_{ab\to VX\to f\bar{f}'X} \ \widetilde{\Gamma_V\to 0} \ \frac{1}{2s_{ab}} \int \mathrm{d}\Phi_{VX}(\hat{k}) \sum_{\lambda,\lambda'=0,\pm1} \mathcal{M}_{ab\to VX}(\lambda')^* \mathcal{M}_{ab\to VX}(\lambda)$$

$$\times \mathrm{BR}_{V\to f\bar{f}'} \int \frac{\mathrm{d}\Phi_{f\bar{f}'}(\hat{k}_1,\hat{k}_2)}{\Phi_{f\bar{f}'}} \underbrace{\Delta_{\lambda'\lambda}^{V\to f\bar{f}'}(\hat{k}_1,\hat{k}_2)}_{\text{decay correlation matrix}},$$

$$\Delta_{\lambda'\lambda}^{V\to f\bar{f}'}(\hat{k}_1,\hat{k}_2) = \frac{\Phi_{f\bar{f}'}}{2M_V\Gamma_{V\to f\bar{f}'}} \mathcal{M}_{V\to f\bar{f}'}(\lambda')^* \mathcal{M}_{V\to f\bar{f}'}(\lambda).$$

W decays via improved NWA

Two different (equivalent) implementation strategies

$\hat{k} = \hat{k}_1 + \hat{k}_2, \; \hat{k}^2 = M_V^2$

- Decay correlation matrix

$$\sigma_{ab\to VX\to f\bar{f}'X} \;\widetilde{\Gamma_V\to 0}\; \frac{1}{2s_{ab}} \int d\Phi_{VX}(\hat{k}) \sum_{\lambda,\lambda'=0,\pm1} \mathcal{M}_{ab\to VX}(\lambda')^* \mathcal{M}_{ab\to VX}(\lambda)$$

$$\times \mathrm{BR}_{V\to f\bar{f}'} \int \frac{d\Phi_{f\bar{f}'}(\hat{k}_1,\hat{k}_2)}{\Phi_{f\bar{f}'}} \underbrace{\Delta^{V\to f\bar{f}'}_{\lambda'\lambda}(\hat{k}_1,\hat{k}_2)}_{\text{decay correlation matrix}},$$

$$\Delta^{V\to f\bar{f}'}_{\lambda'\lambda}(\hat{k}_1,\hat{k}_2) = \frac{\Phi_{f\bar{f}'}}{2M_V\Gamma_{V\to f\bar{f}'}} \mathcal{M}_{V\to f\bar{f}'}(\lambda')^* \mathcal{M}_{V\to f\bar{f}'}(\lambda).$$

- Replacement of polarization vectors by leptonic currents in the amplitude

$$\sigma_{ab\to VX\to f\bar{f}'X} \;\widetilde{\Gamma_V\to 0}\; \frac{1}{2s_{ab}} \int d\Phi_{VX}(\hat{k}) \int \frac{d\Phi_{f\bar{f}'}(\hat{k}_1,\hat{k}_2)}{2M_V\Gamma_V} \sum_{\sigma=\pm1} |\tilde{\mathcal{M}}_{ab\to V(\to f\bar{f}')X}(\sigma)|^2,$$

$\tilde{\mathcal{M}}_{ab\to V(\to f\bar{f}')X}(\sigma) = \mathcal{M}_{ab\to VX}(\lambda)$ with

$$\varepsilon_V^{*\mu}(\lambda) \longrightarrow \tilde{\varepsilon}^{*\mu}_{V\to f\bar{f}'}(\sigma) = e\, g^{\sigma}_{Vff'}\, \bar{u}_f(\hat{k}_1)\gamma^\mu\omega_\sigma v_{\bar{f}'}(\hat{k}_2).$$

Full calculation vs. sNWA vs. iNWA at LO at LHC

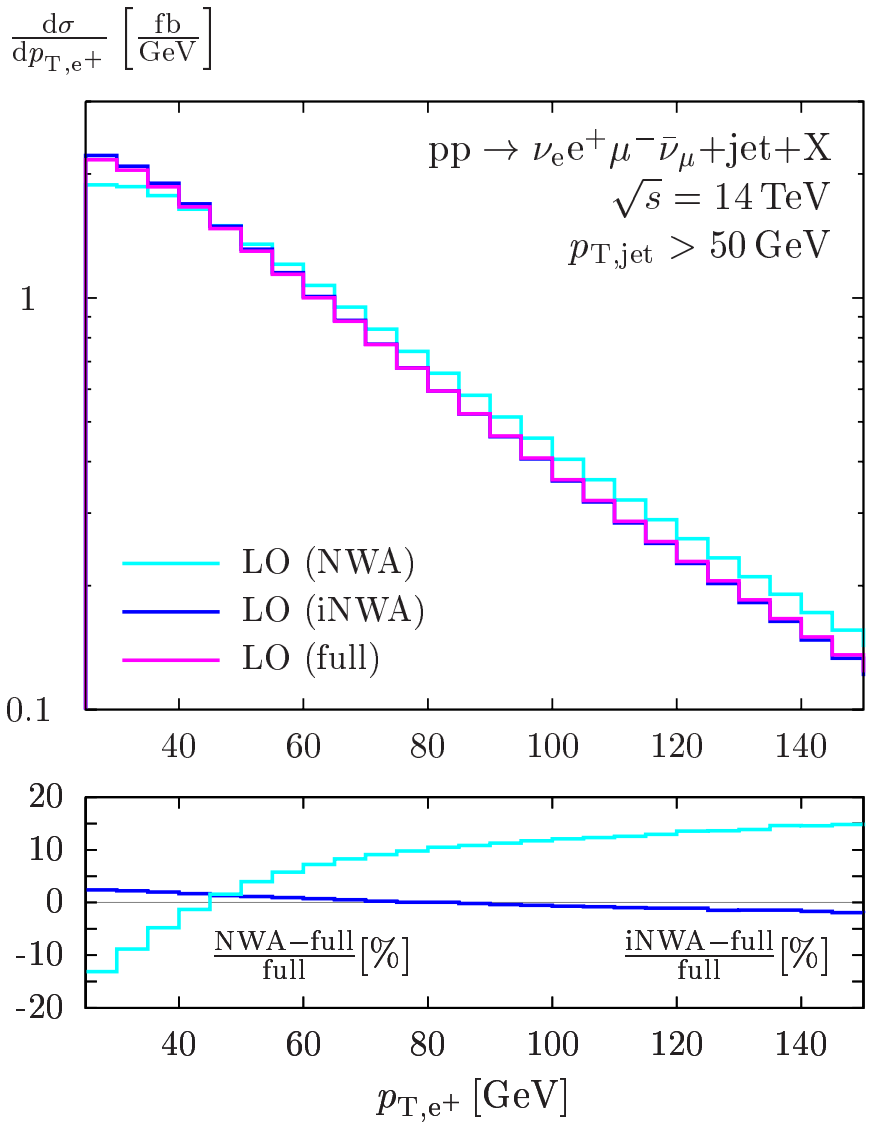

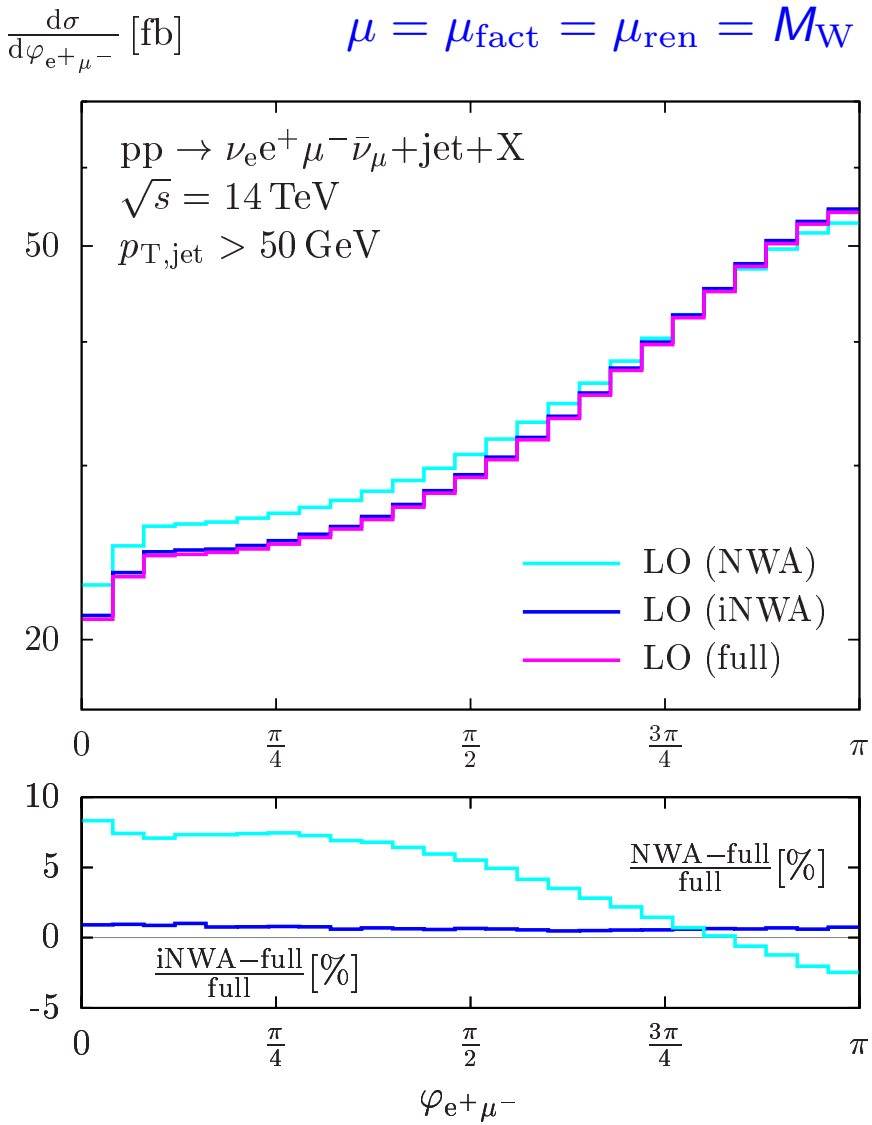

Full calculation vs. sNWA vs. iNWA at LO at Tevatron

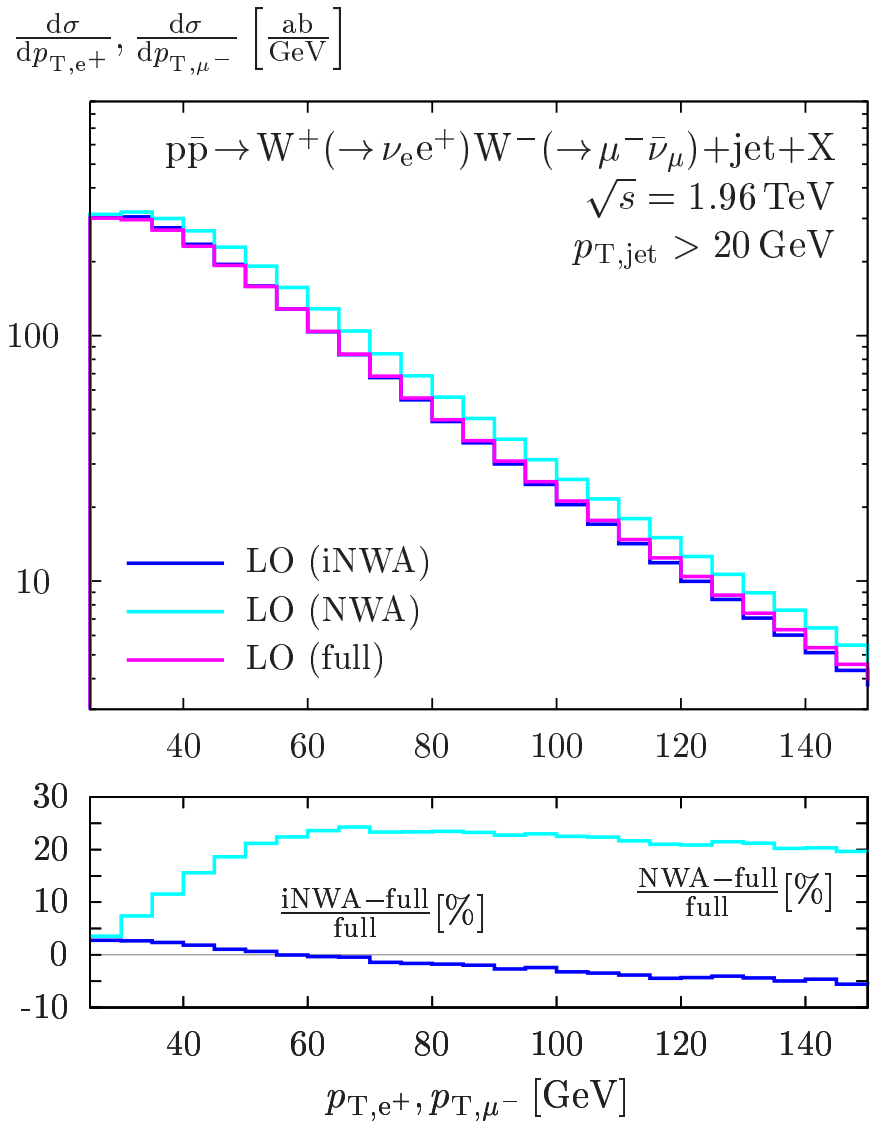

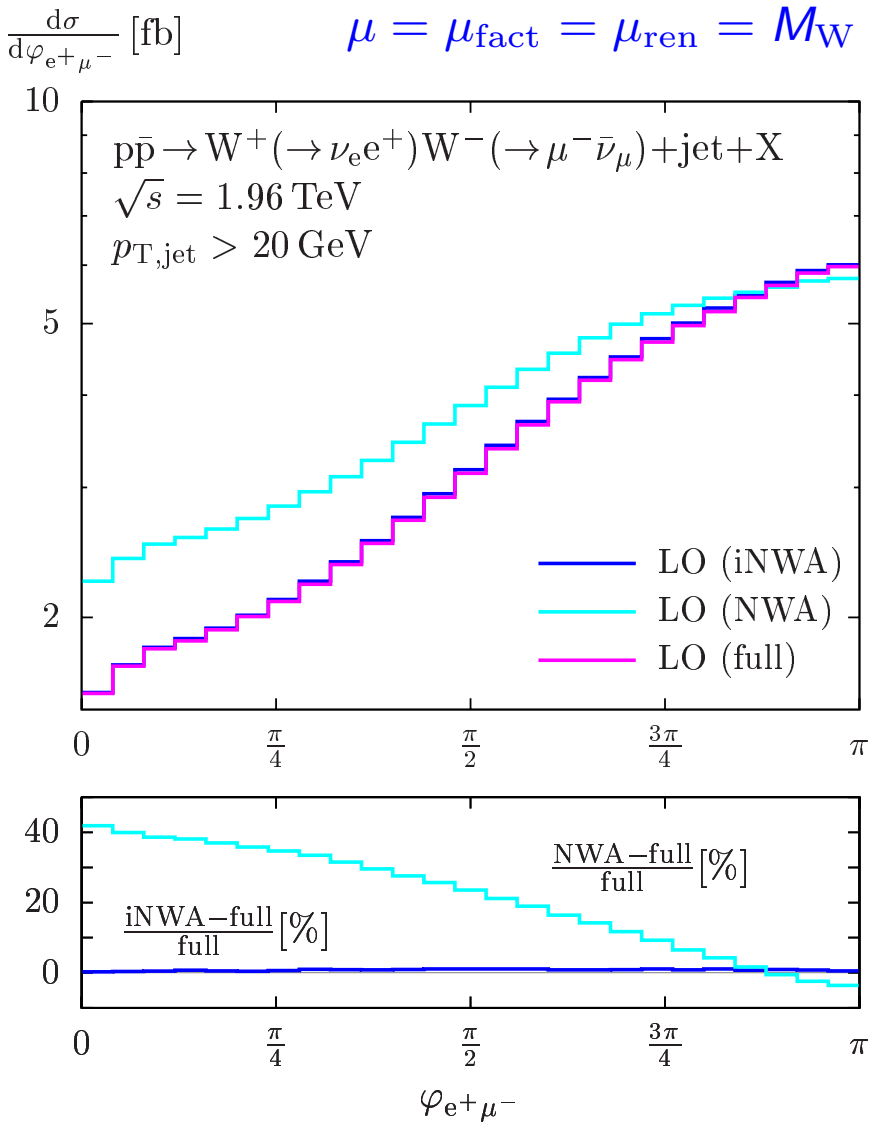

Scale dependence of cross sections at the LHC

LO versus NLO cross sections with stable W bosons:

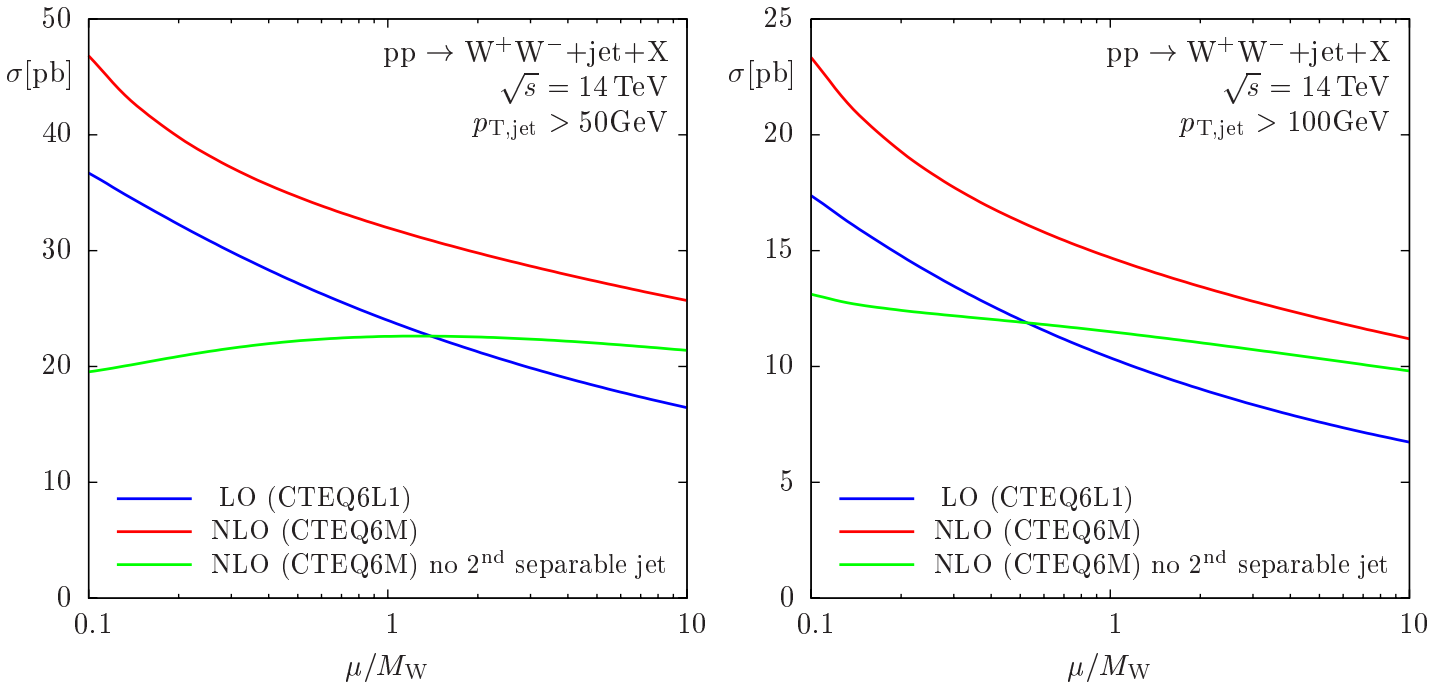

$\mu = \mu_{\text{fact}} = \mu_{\text{ren}}$

Jet definition: successive combination algorithm (with $R = 1$) [S.D.Ellis, Soper '93]

- Scale dependence stabilizes at NLO for genuine WW+jet production.
- But: Significant scale dependence is introduced by WW+2jets events.

Scale dependence of cross sections at the LHC

LO versus NLO cross sections including leptonic W decays via improved NWA:

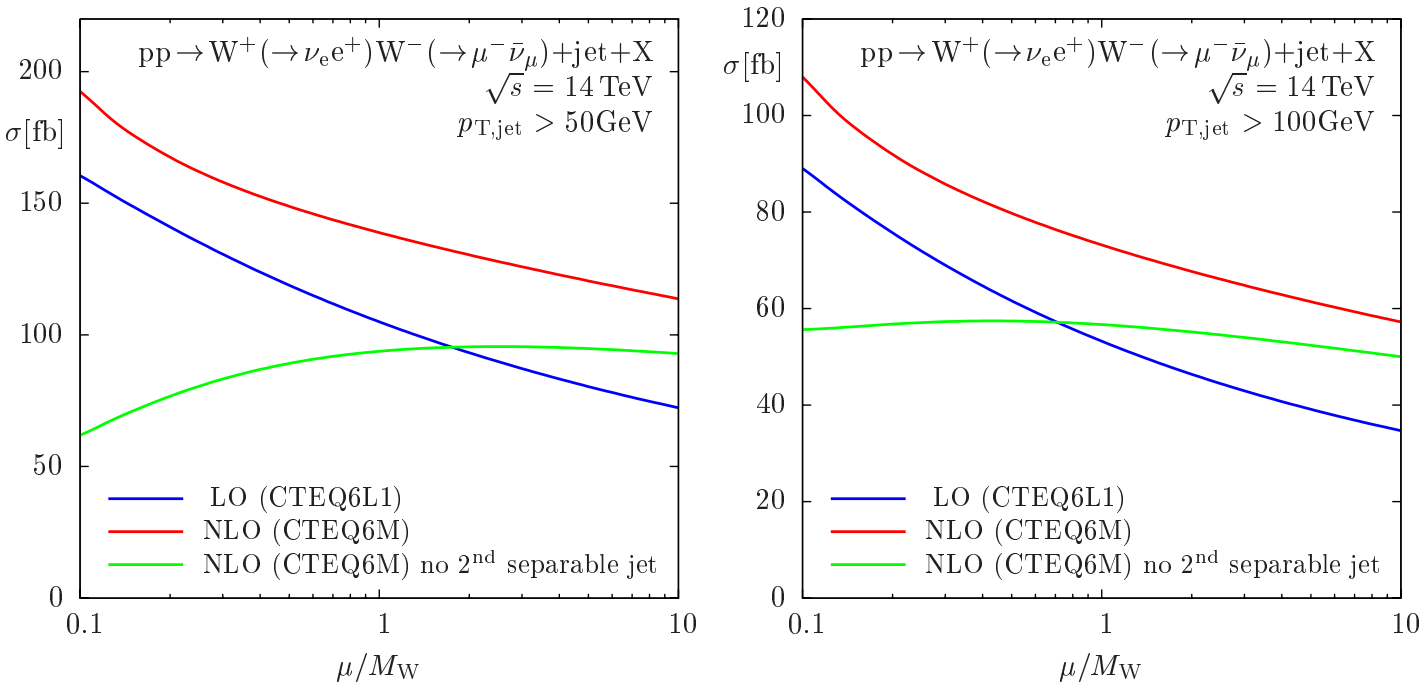

$\mu = \mu_{\text{fact}} = \mu_{\text{ren}}$

Additional cuts:

$|\eta_{\text{jet}}| < 4.5$
$p_{T,\text{lep}} > 25\,\text{GeV}$
$|\eta_{\text{lep}}| < 2.5$
$p_{T,\text{miss}} > 25\,\text{GeV}$
$R_{\text{jet,lep}} > 0.4$
$R_{\text{lep,lep}} > 0.2$

Jet definition: successive combination algorithm (with $R = 1$) [S.D.Ellis, Soper '93]

- Scale dependence stabilizes at NLO for genuine WW+jet production.
- But: Significant scale dependence is introduced by WW+2jets events.

Scale dependence of cross sections at the Tevatron

LO versus NLO cross sections with stable W bosons:

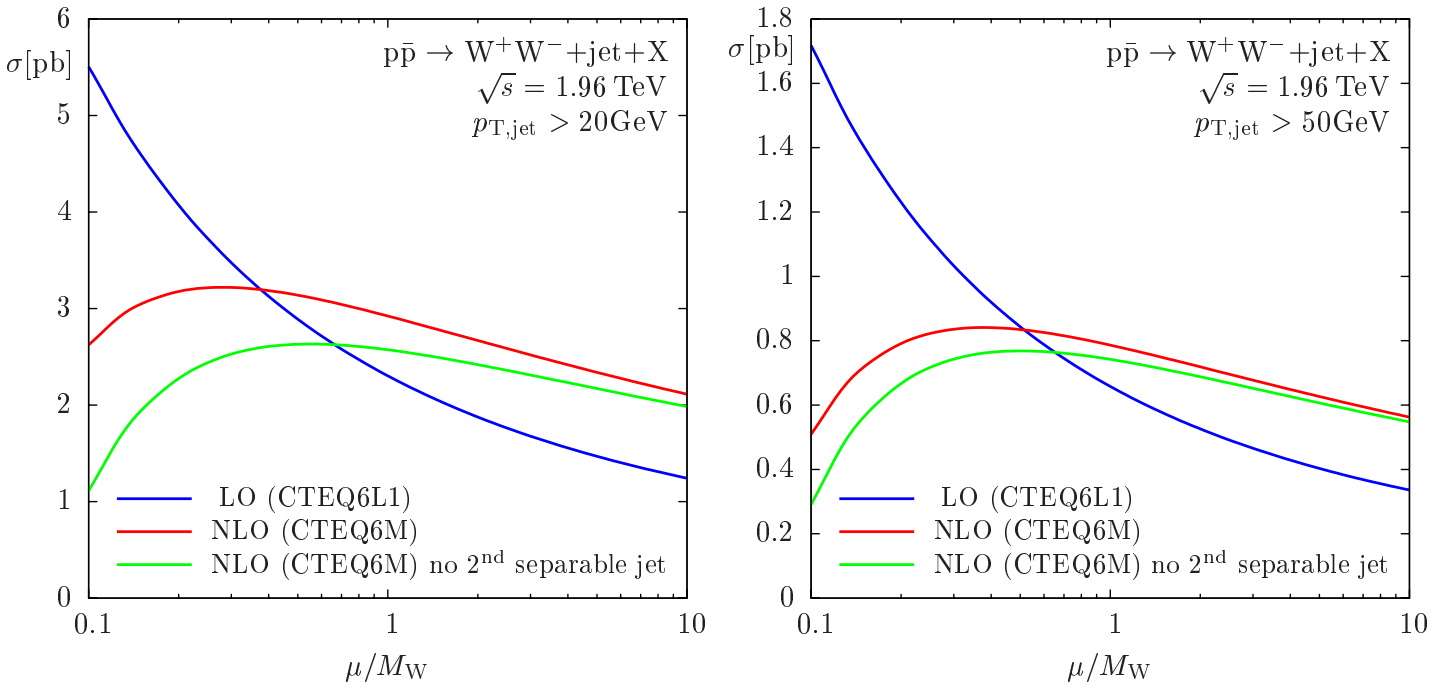

$\mu = \mu_{\text{fact}} = \mu_{\text{ren}}$

Jet definition: successive combination algorithm (with $R = 1$) [S.D.Ellis, Soper '93]

- Scale dependence stabilizes at NLO.
- Only small influence from WW+2jets production.

Scale dependence of cross sections at the Tevatron

LO versus NLO cross sections including leptonic W decays via improved NWA:

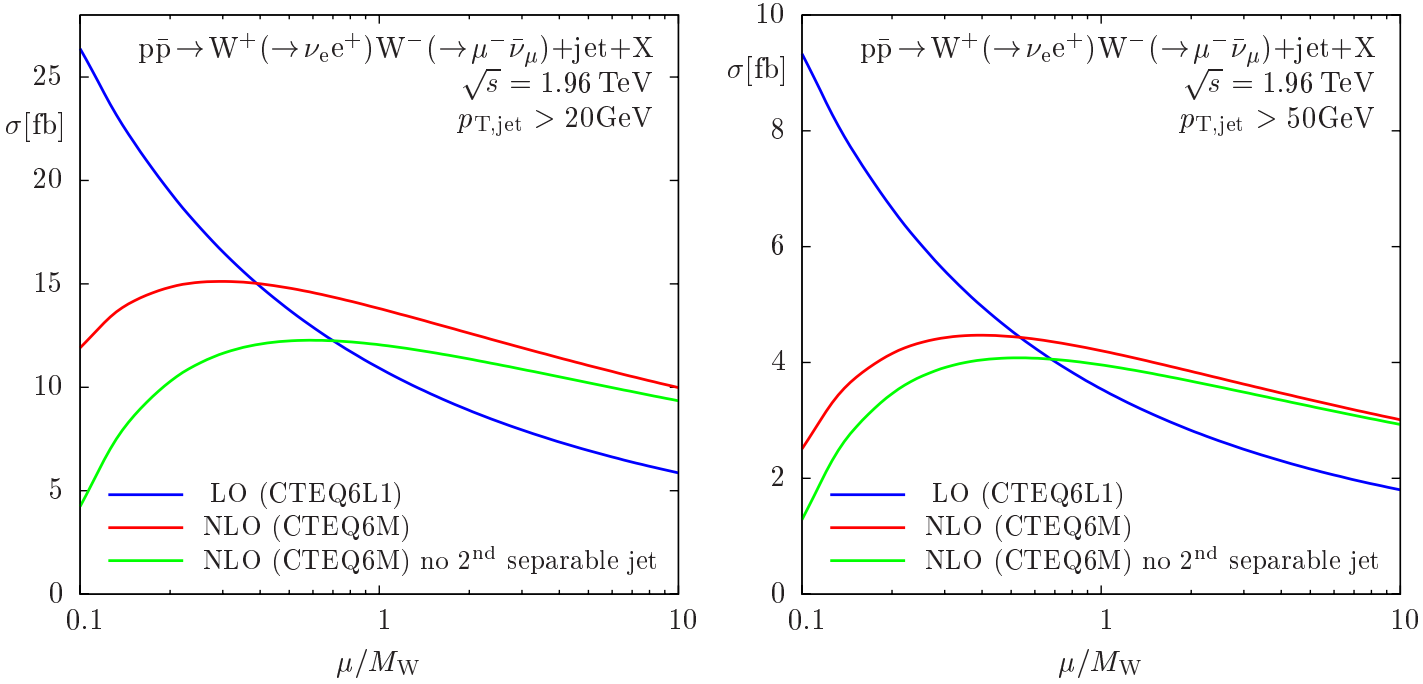

$\mu = \mu_{\text{fact}} = \mu_{\text{ren}}$

Additional cuts:

$|\eta_{\text{jet}}| < 4.5$
$p_{T,\text{lep}} > 25\,\text{GeV}$
$|\eta_{\text{lep}}| < 2.5$
$p_{T,\text{miss}} > 25\,\text{GeV}$
$R_{\text{jet,lep}} > 0.4$
$R_{\text{lep,lep}} > 0.2$

Jet definition: successive combination algorithm (with $R = 1$) [S.D.Ellis, Soper '93]

- Scale dependence stabilizes at NLO.
- Only small influence from WW+2jets production.

Distributions at LHC: transverse momenta

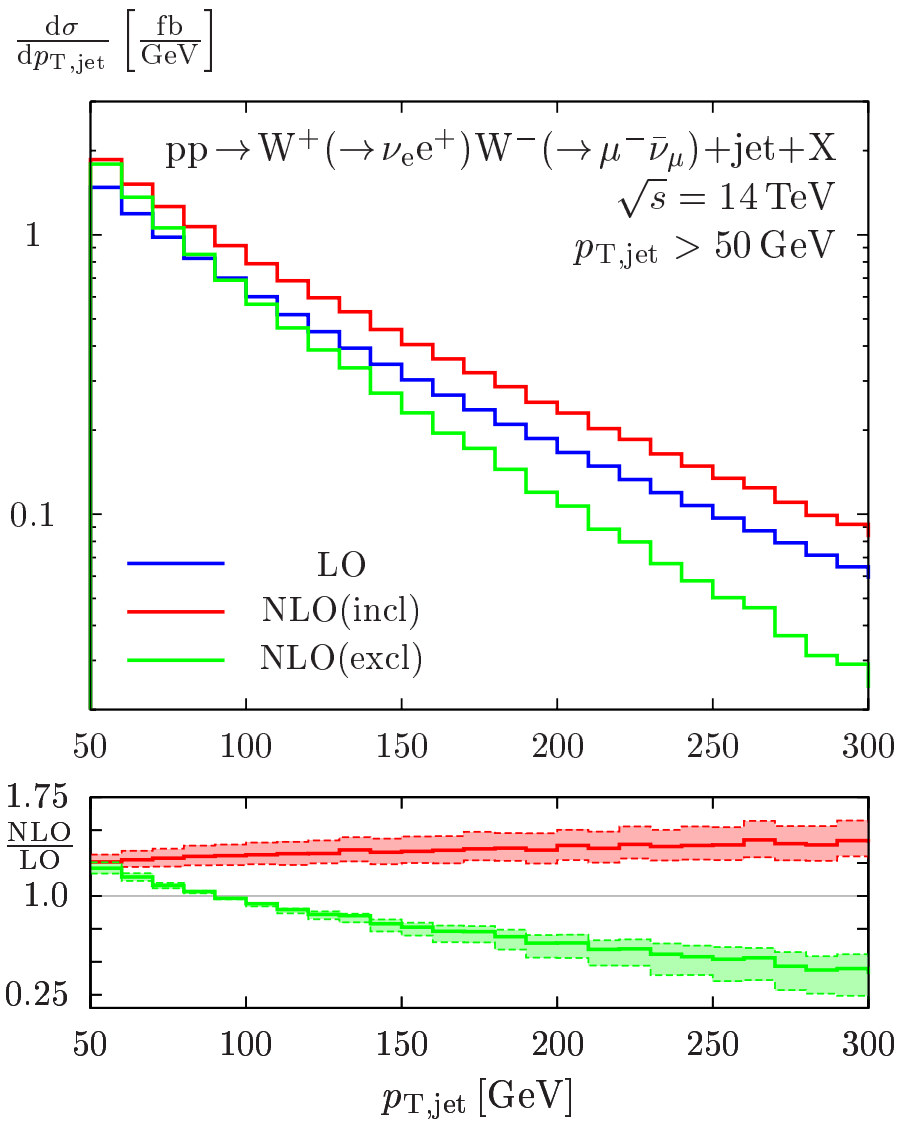

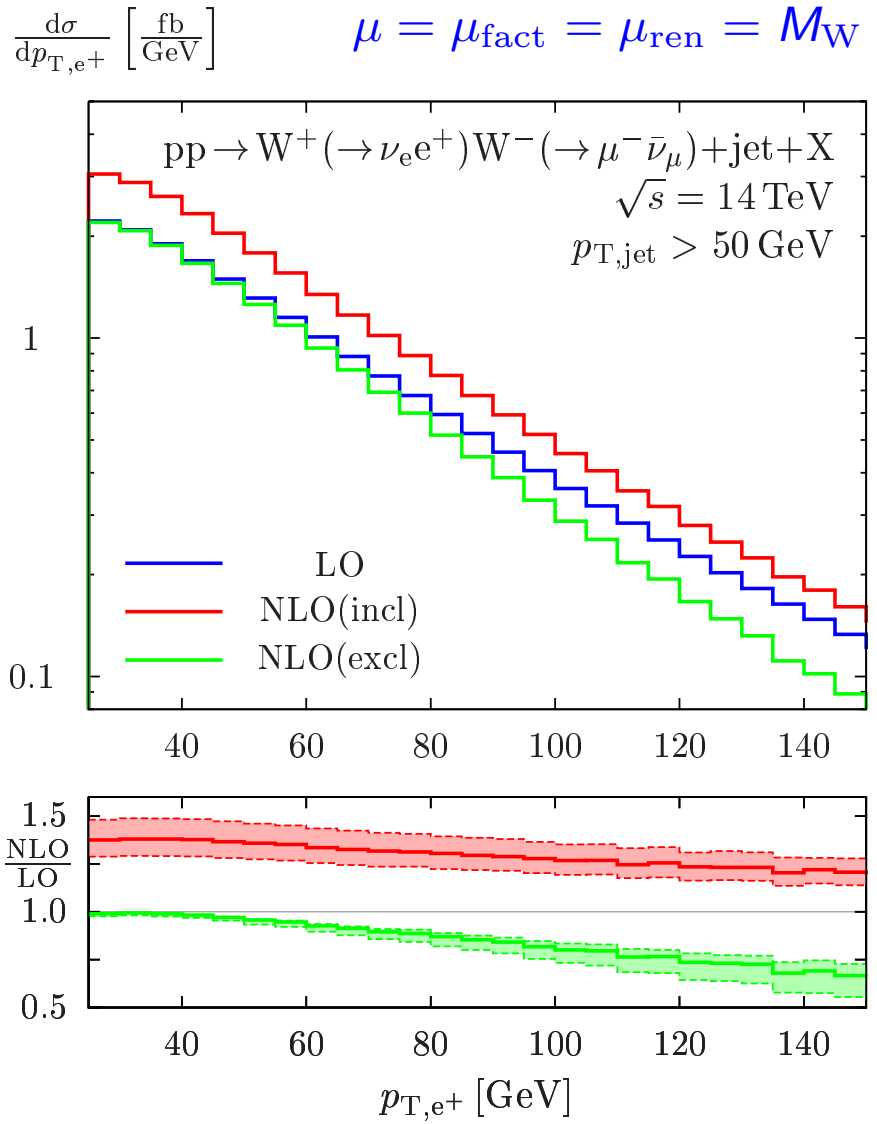

Distributions at LHC: angles between leptons

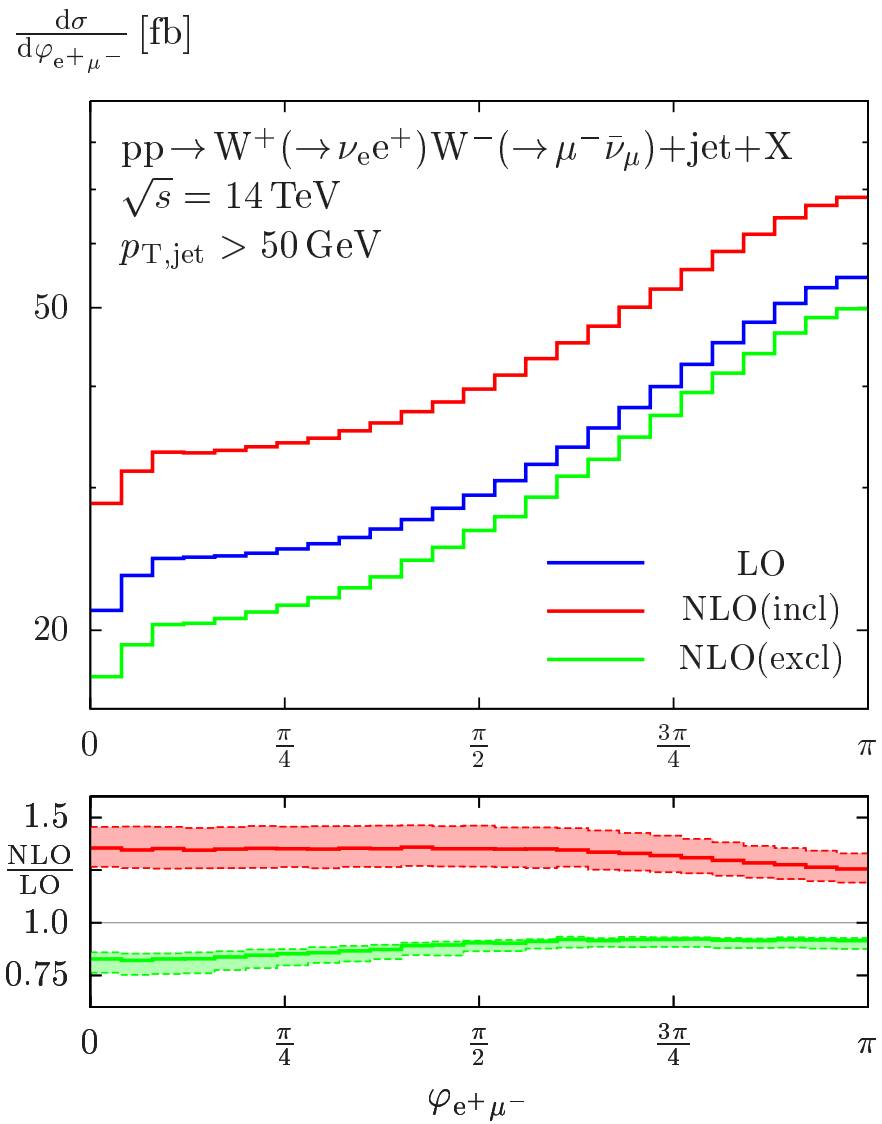

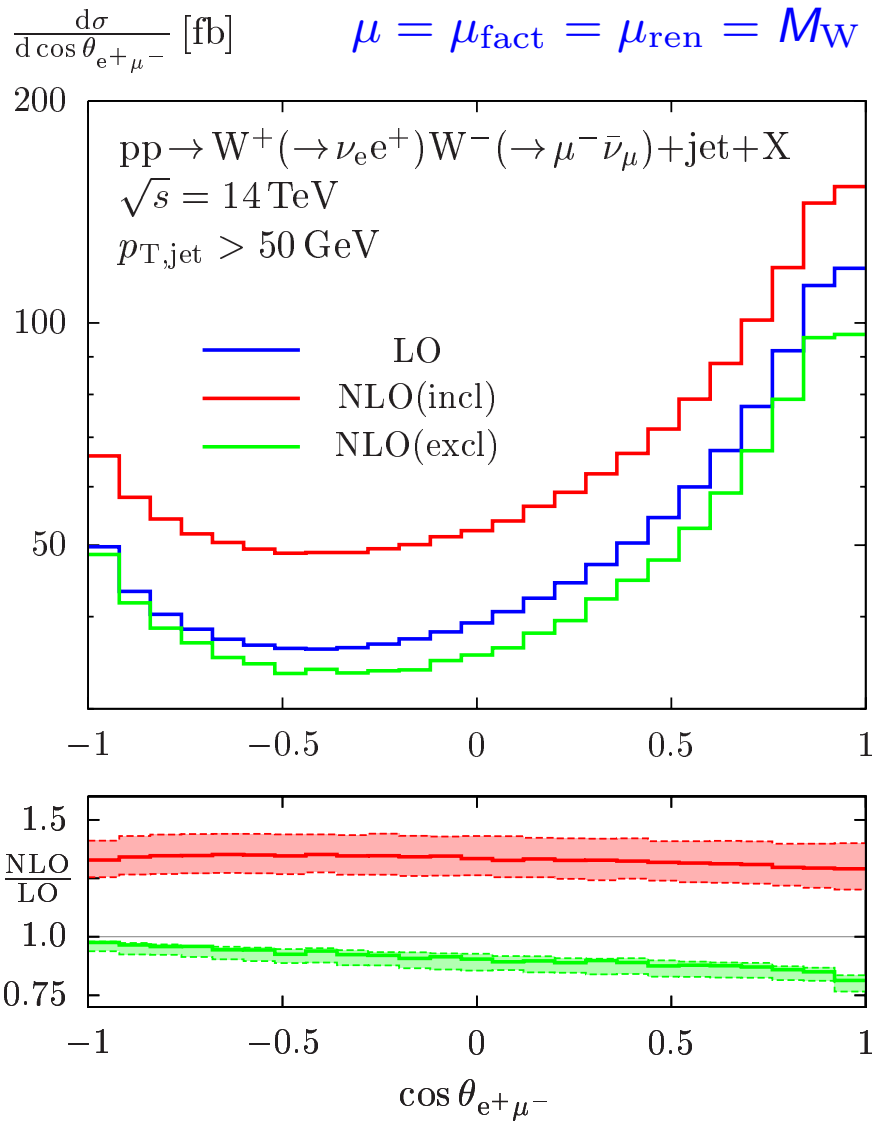

Distributions at Tevatron: transverse momenta

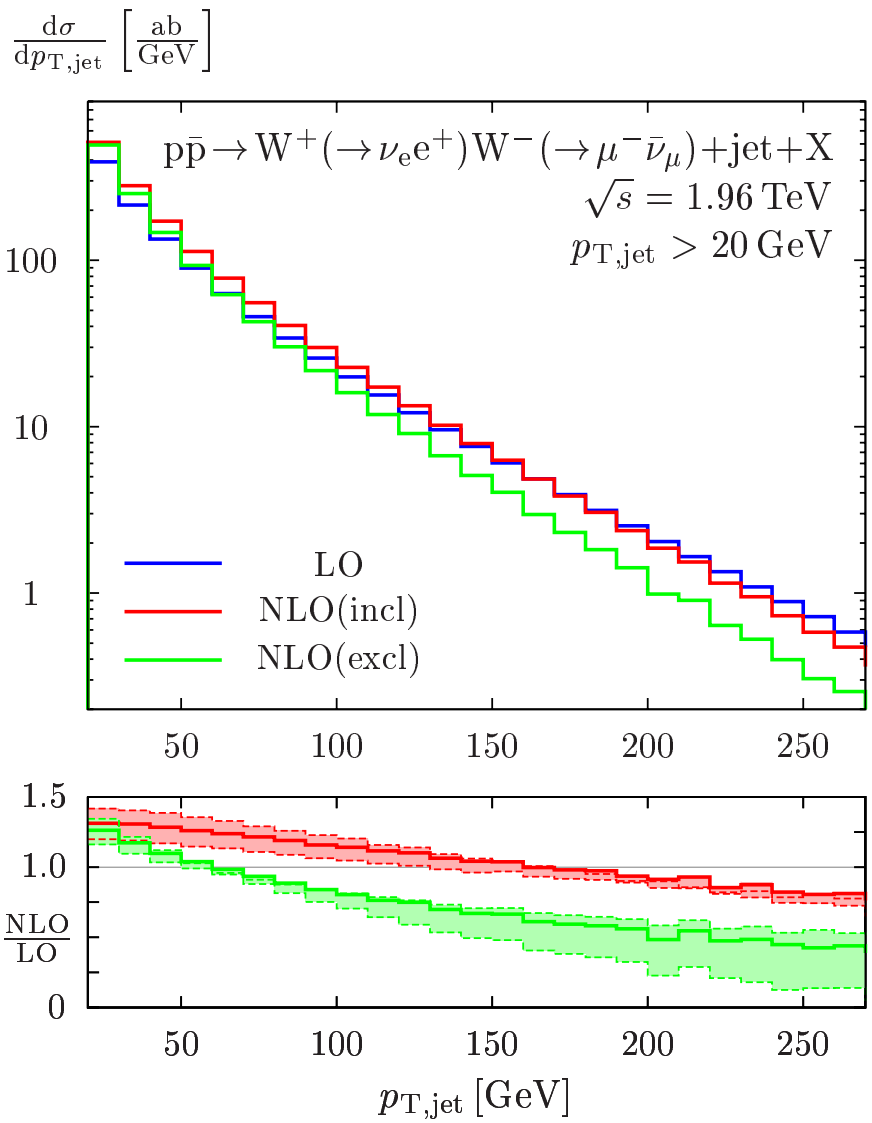

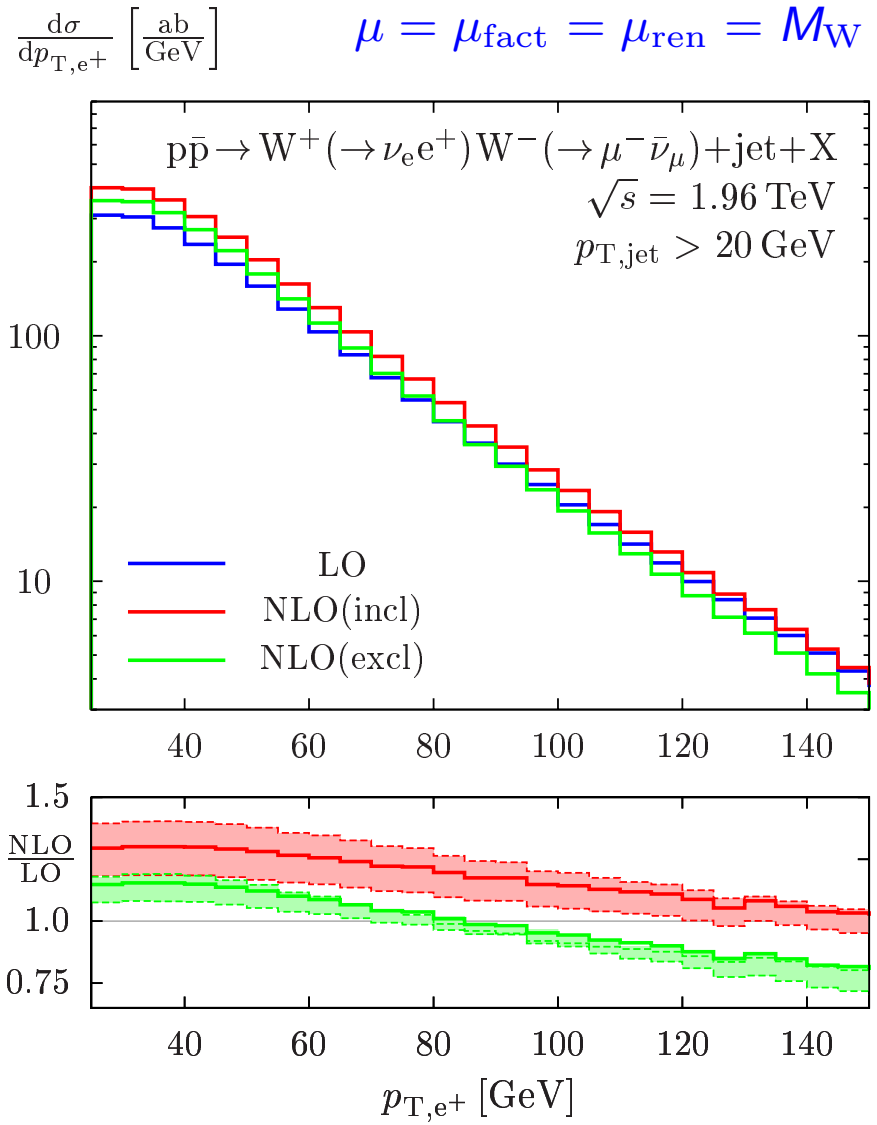

Distributions at Tevatron: angles between leptons

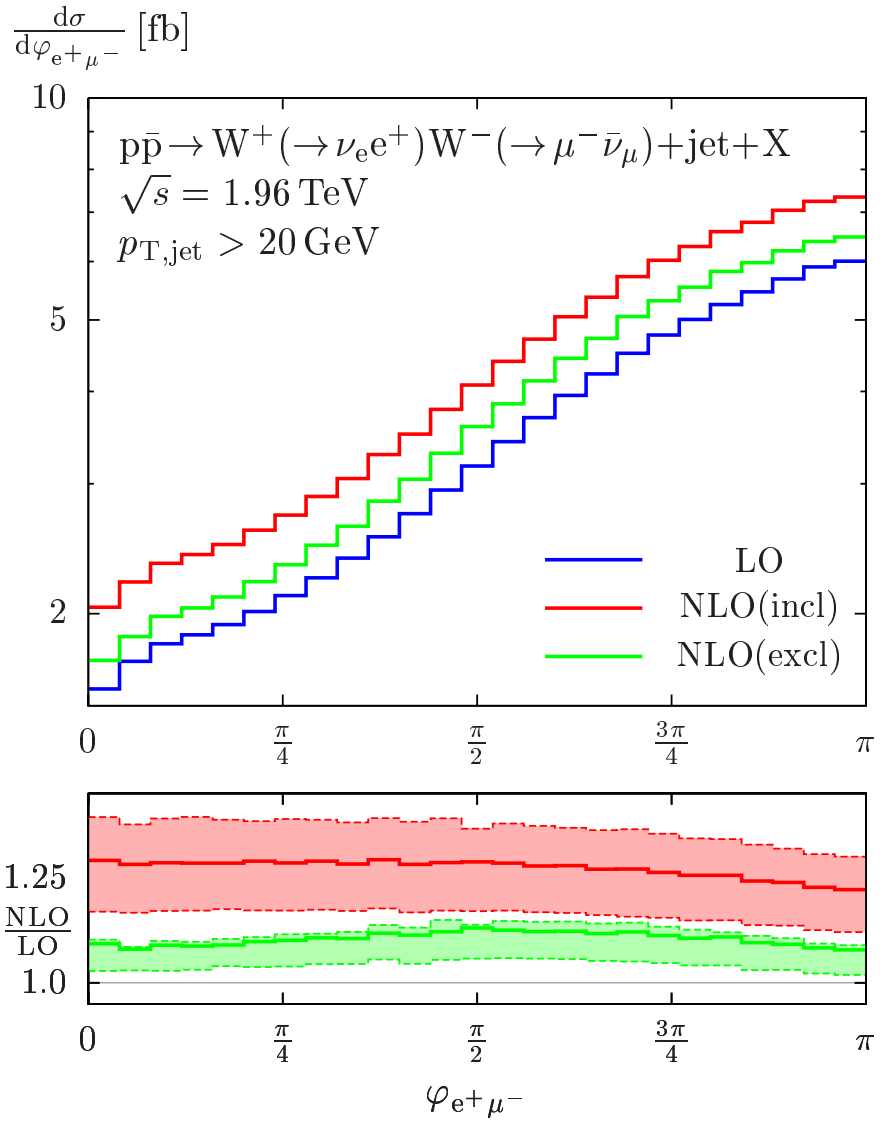

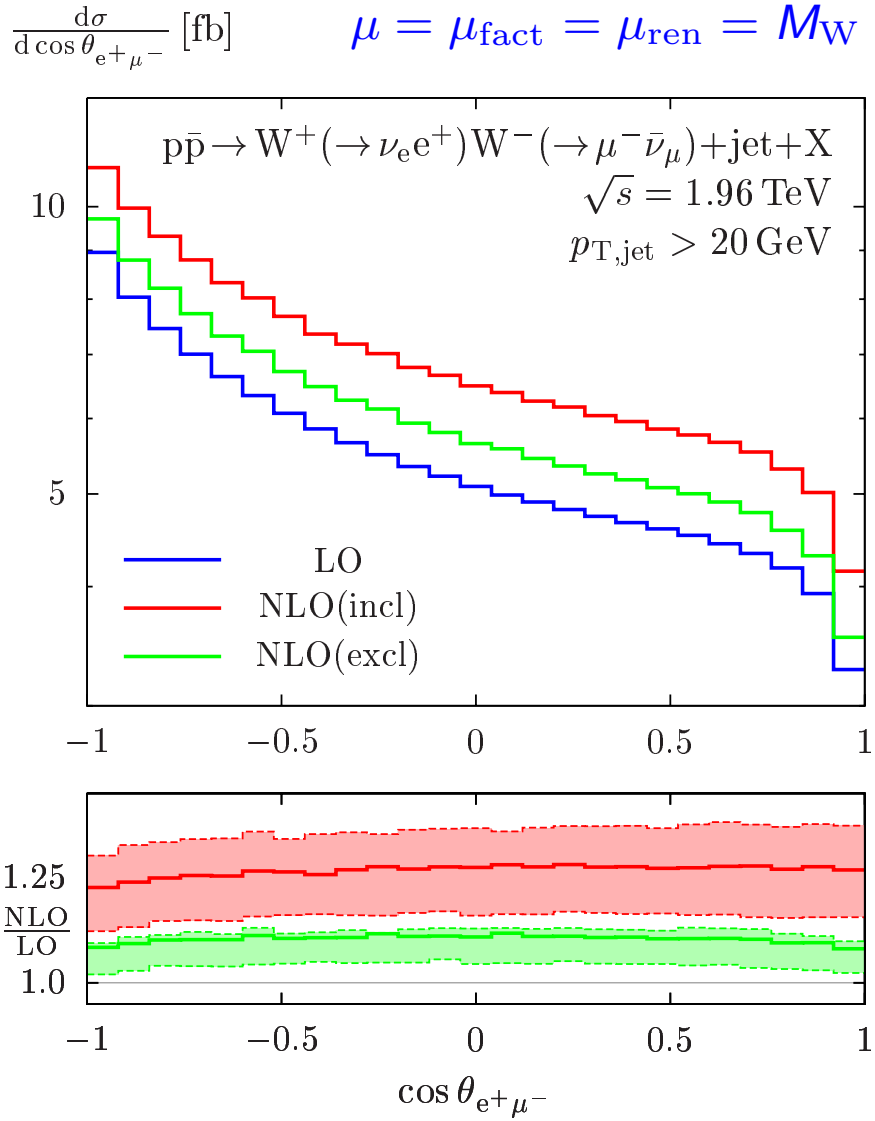

Conclusions & Outlook

Conclusions

$\mathrm{pp}/\mathrm{p\bar{p}} \to \mathrm{WW} + \mathrm{jet} + \mathrm{X}$ at NLO QCD

- Important background process to Higgs and other searches at Tevatron/LHC
- Reduced scale uncertainty at the Tevatron
- Scale dependence at the LHC:
  - Significant reduction for genuine WW+jet production
  - But: significant scale dependence via WW+2jets events
- Leptonic W decays included by means of an improved NWA
- Differential cross sections provided at NLO QCD

Outlook & work in progress

- Calculation of remaining processes of the class $\mathrm{pp}/\mathrm{p\bar{p}} \to \mathrm{VV} + \mathrm{jet} + \mathrm{X}$
- Methods succesfully applied $\longrightarrow$ more complicated applications ($2 \to 4$) feasible!

Backup

Backup slides

Transverse momenta at the LHC

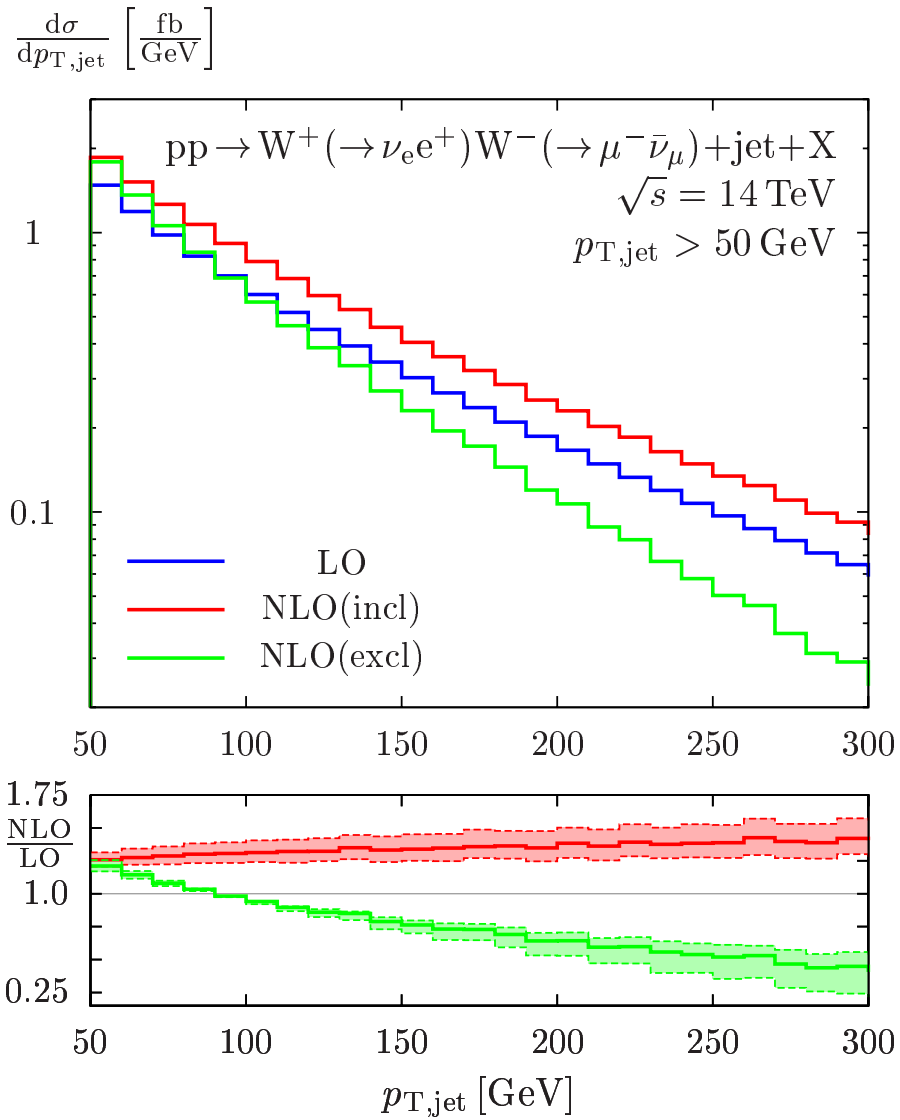

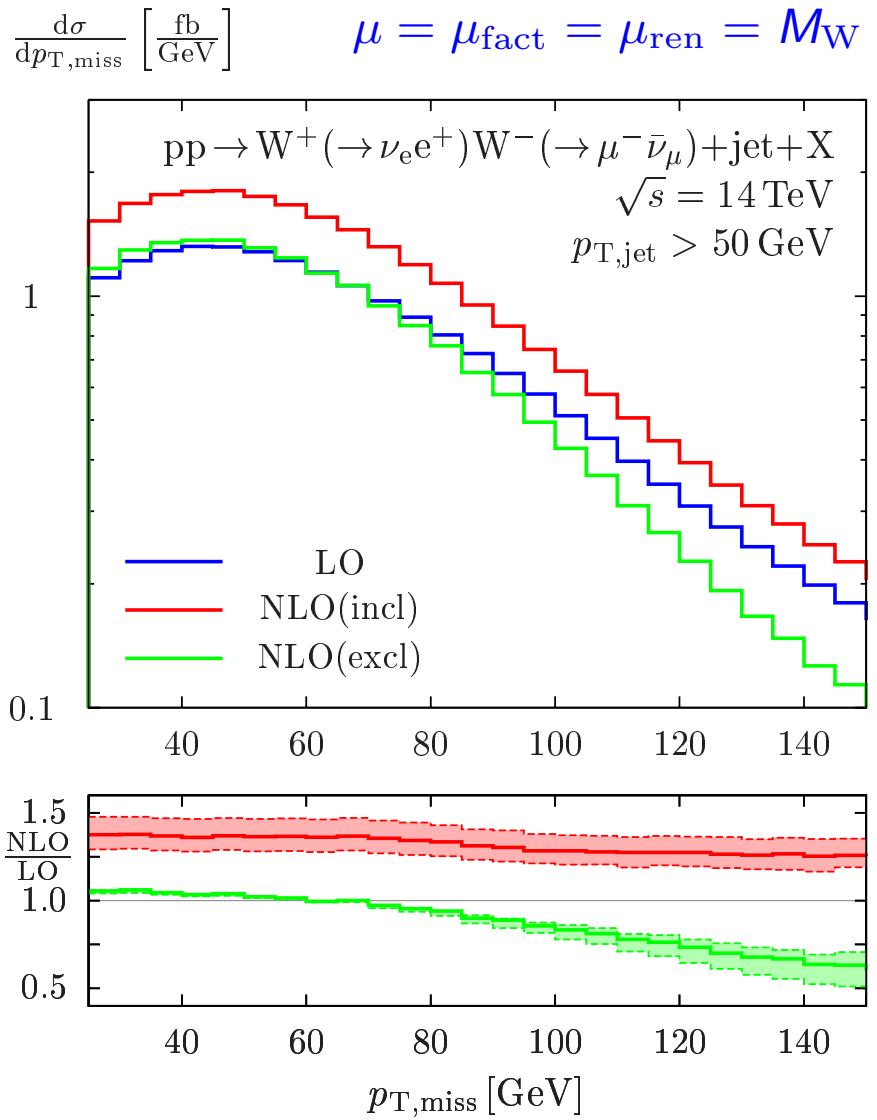

Transverse momenta of leptons at the LHC

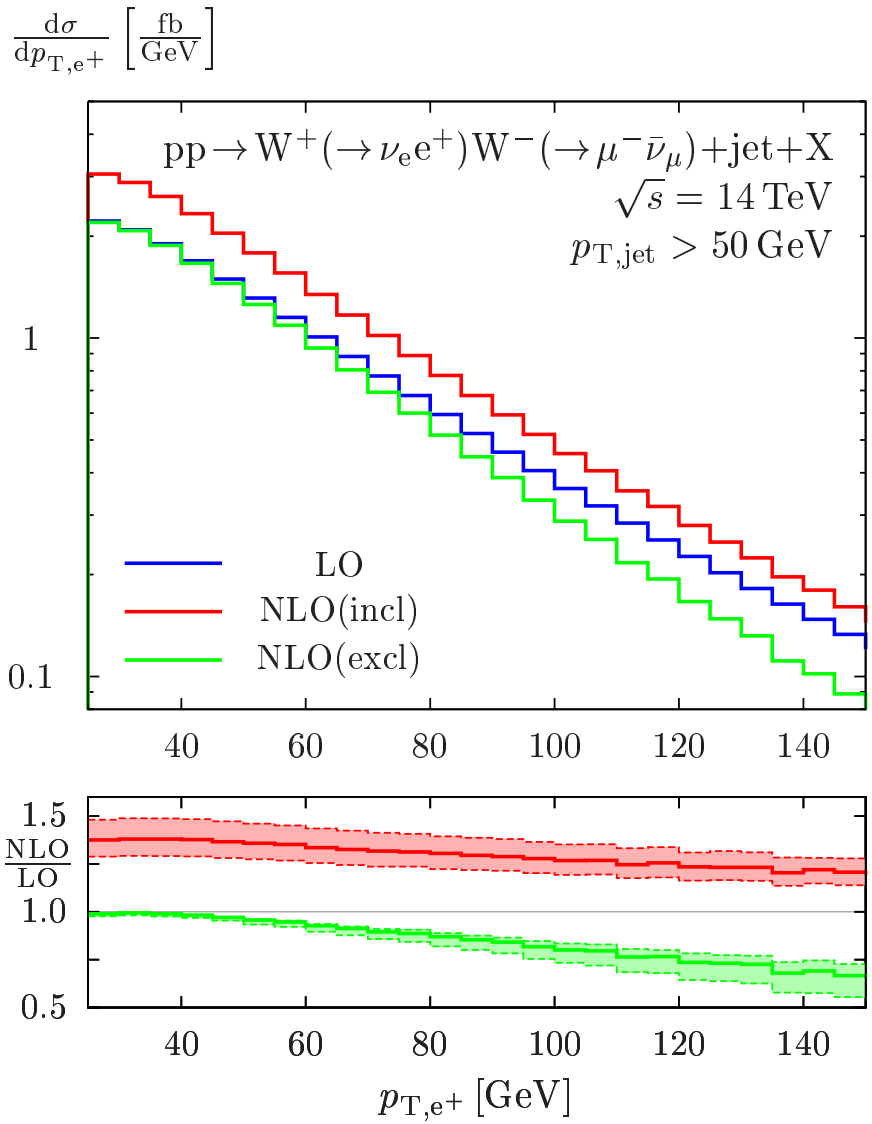

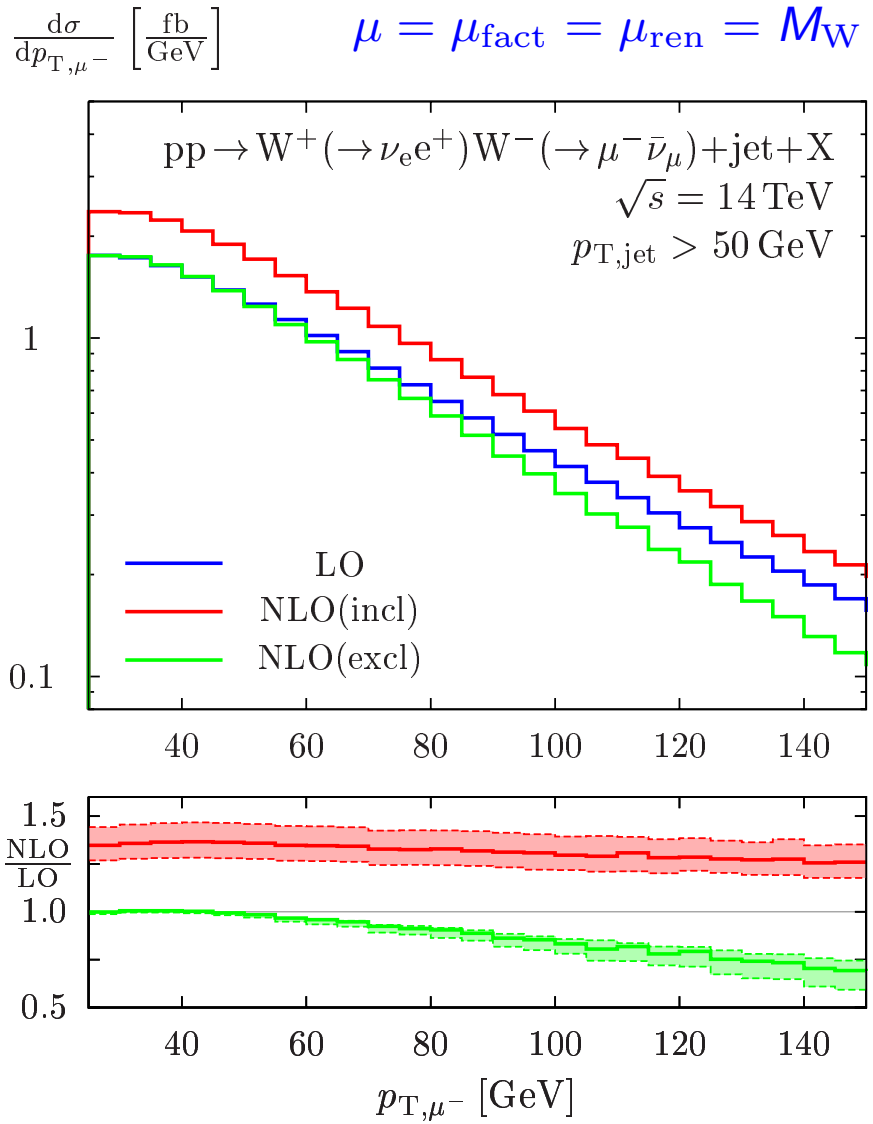

Lepton rapidities at the LHC

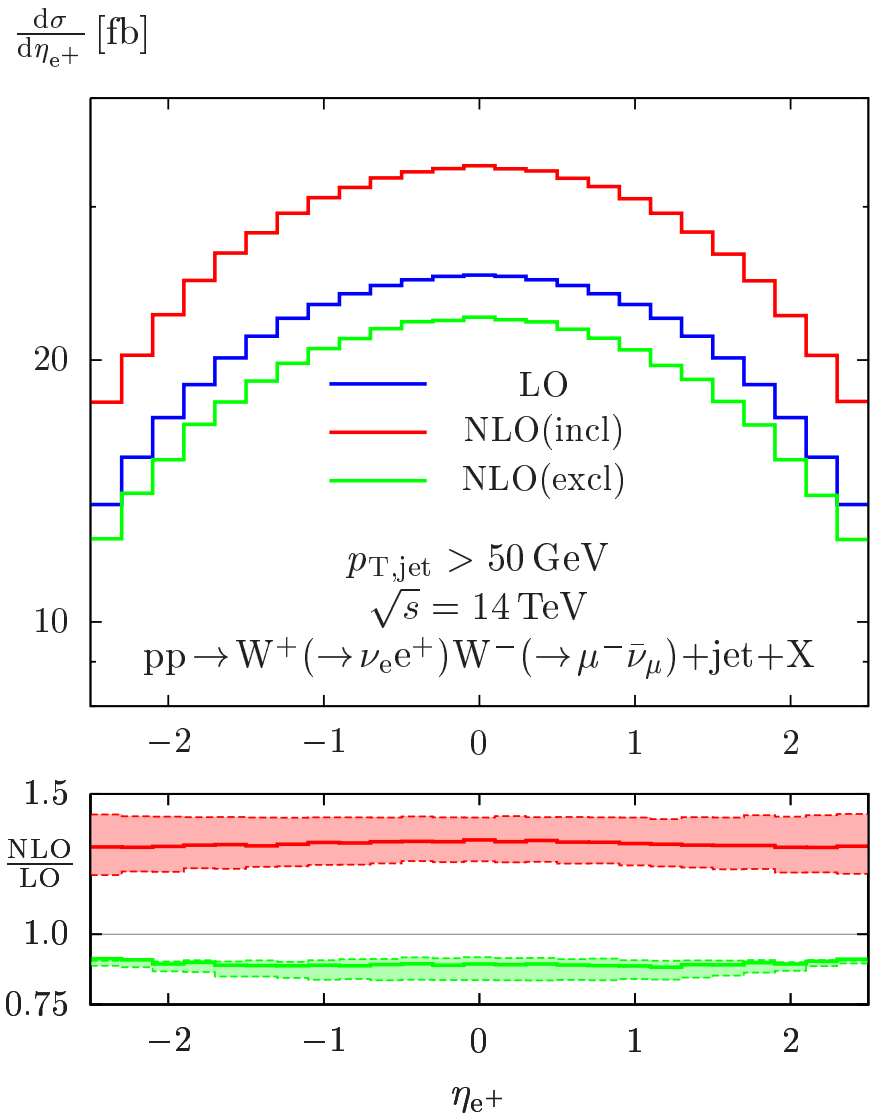

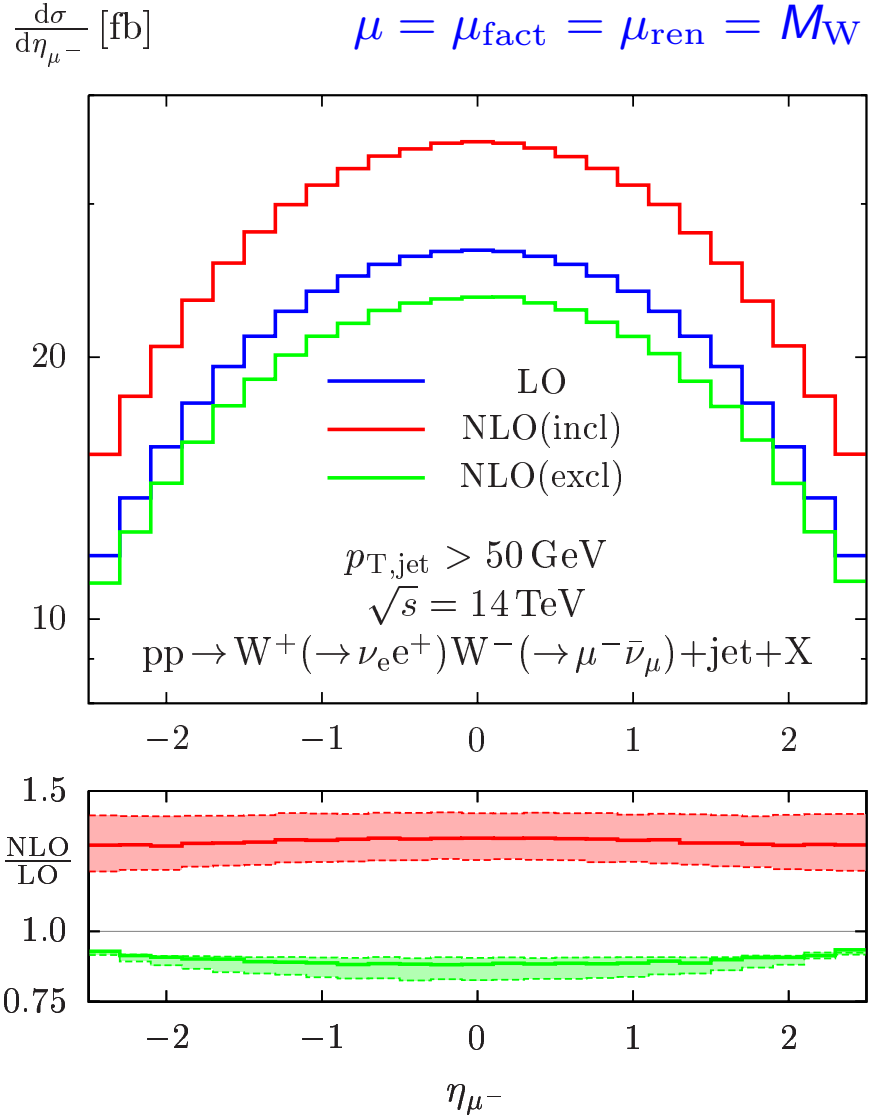

Jet rapidity, invariant mass of leptons at the LHC

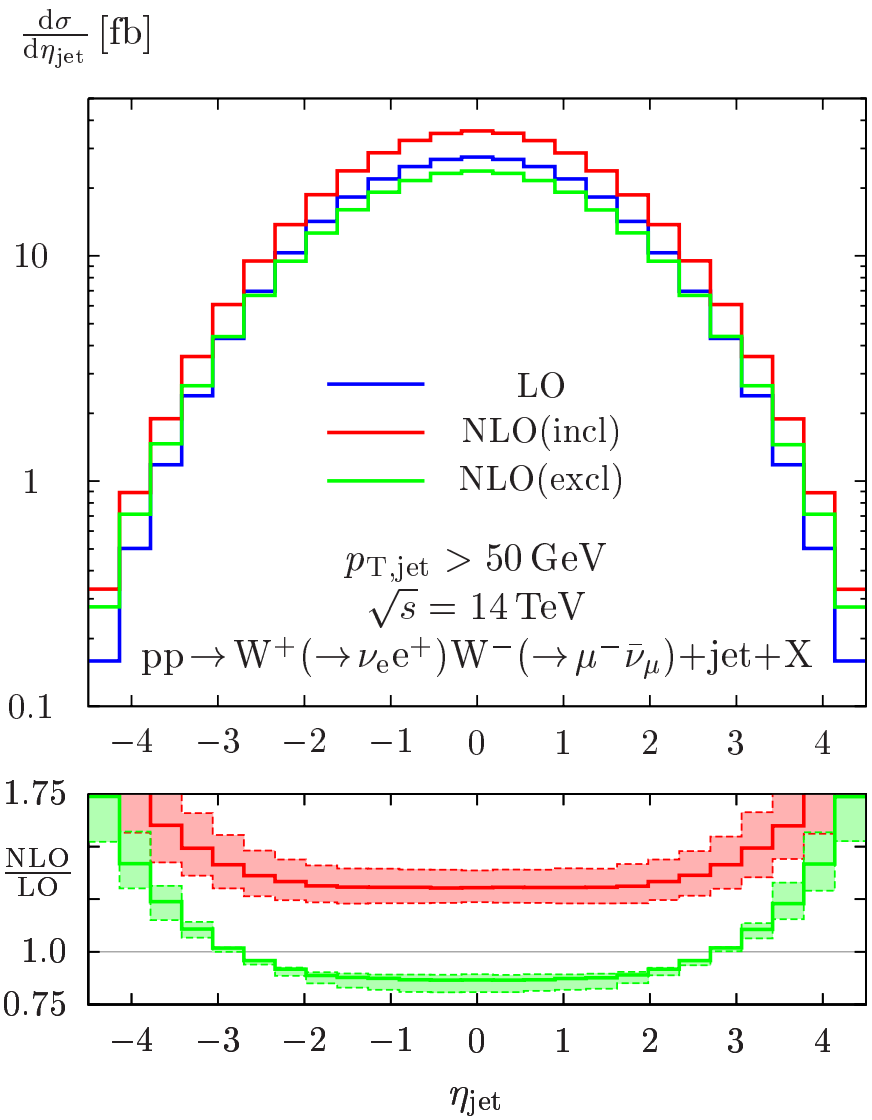

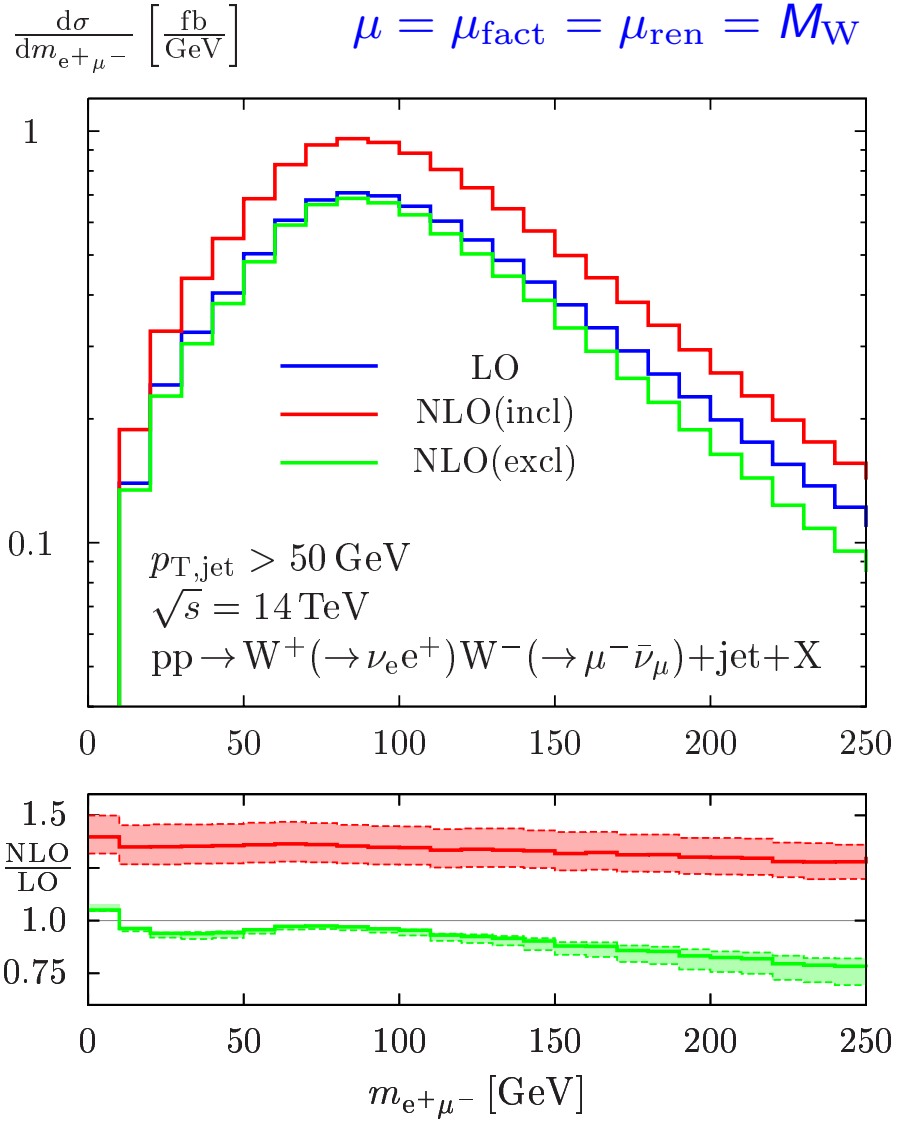

Transverse momenta at the Tevatron

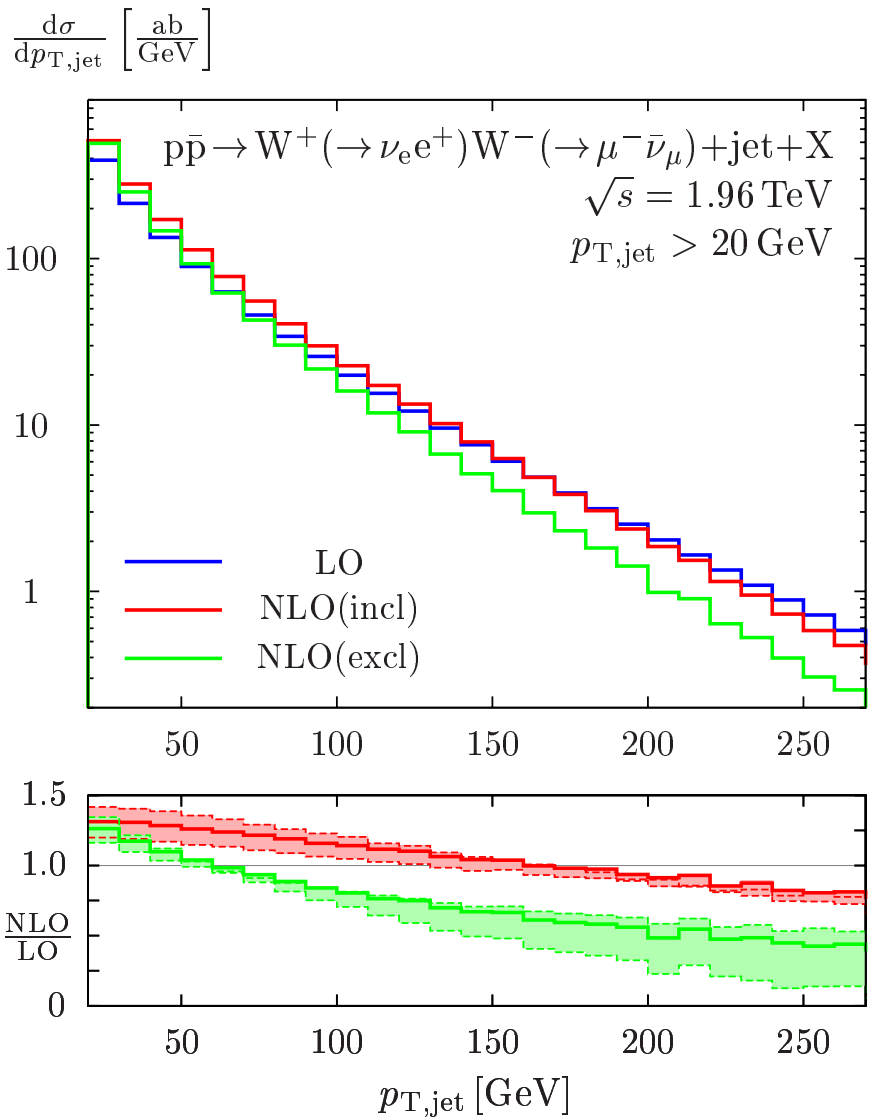

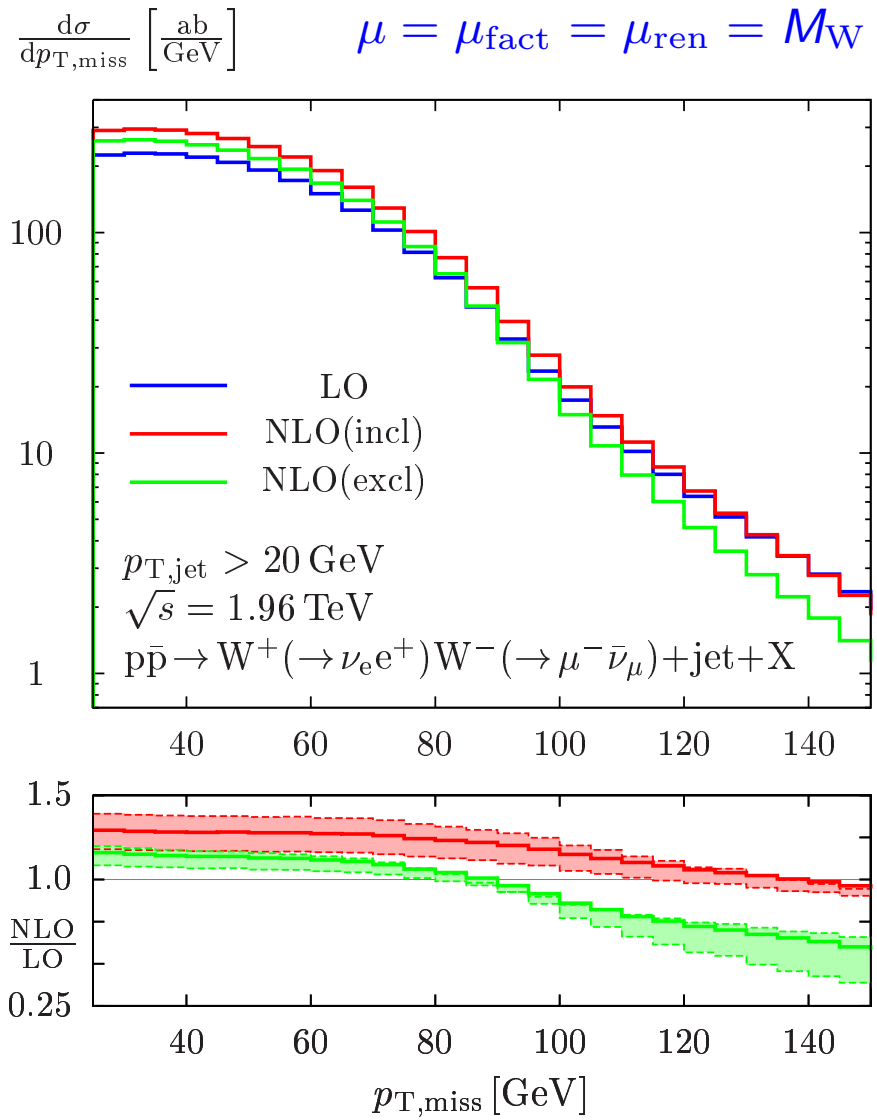

Transverse momenta of leptons at the Tevatron

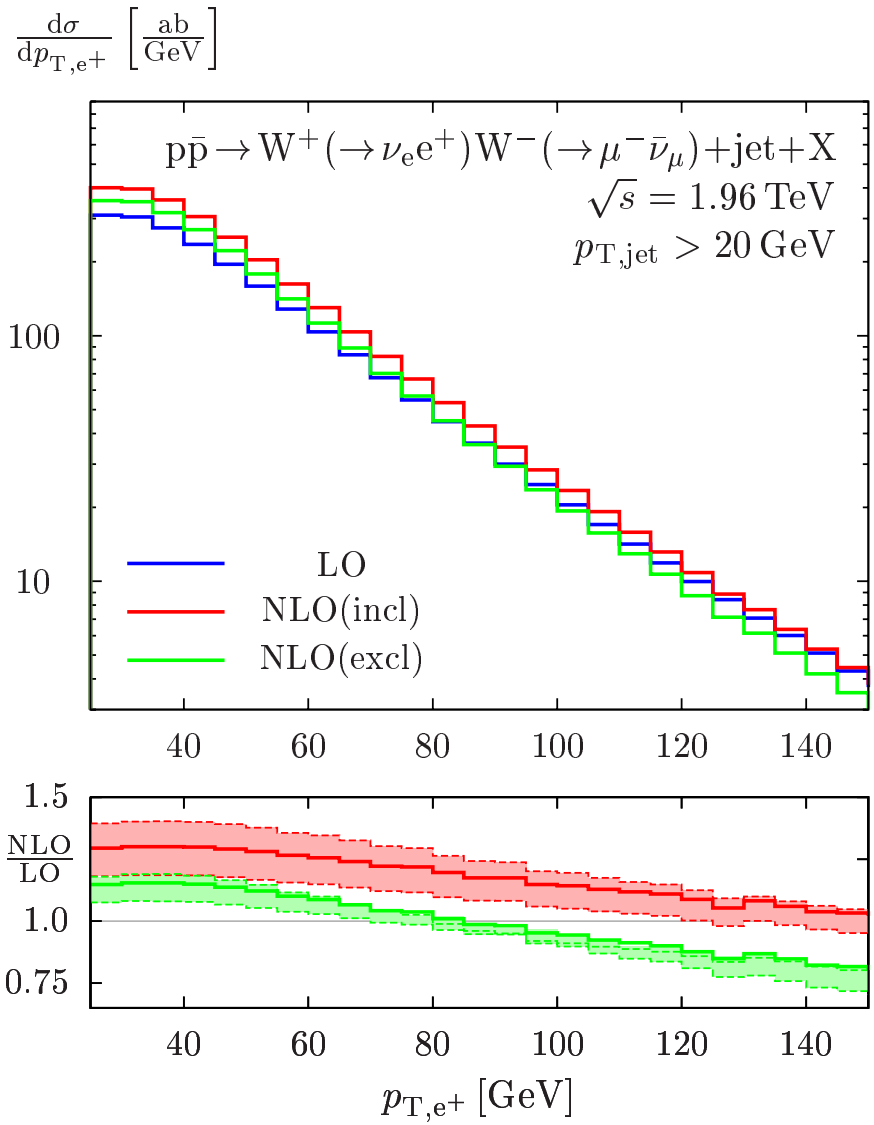

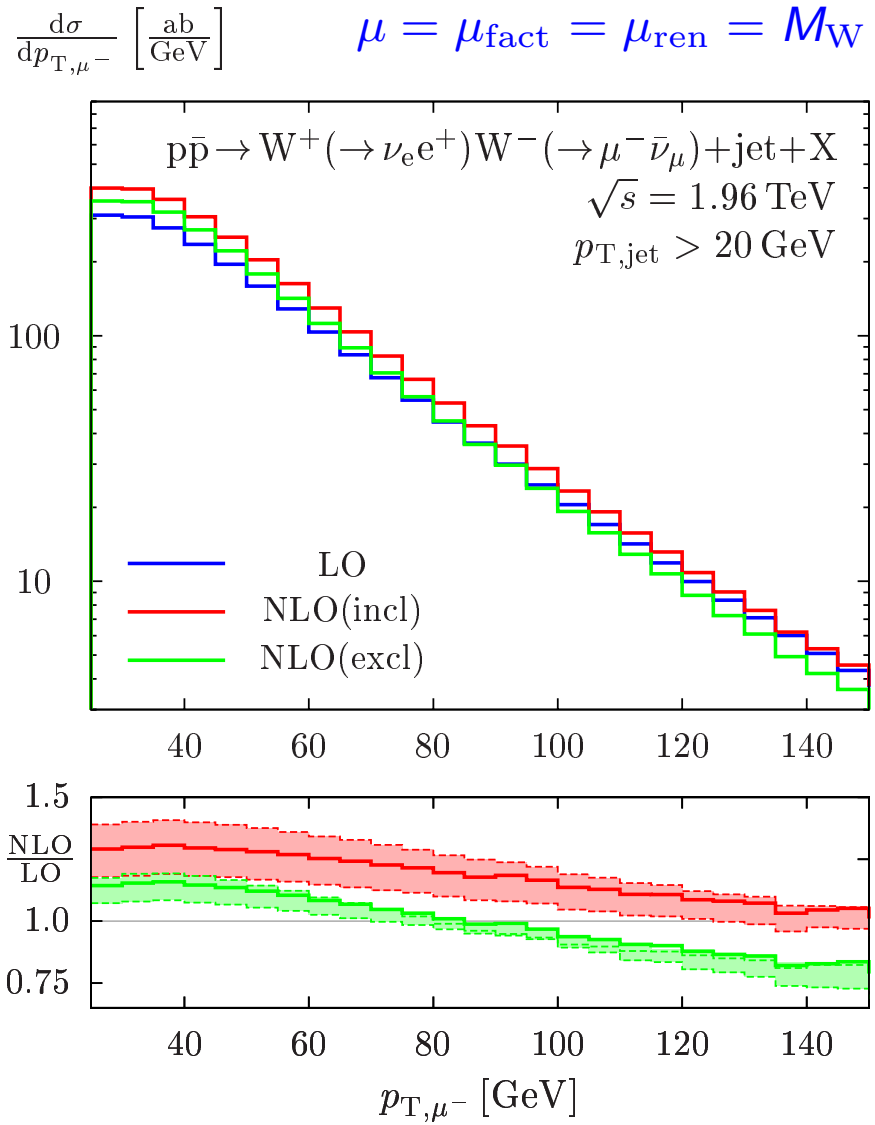

Lepton rapidities at the Tevatron

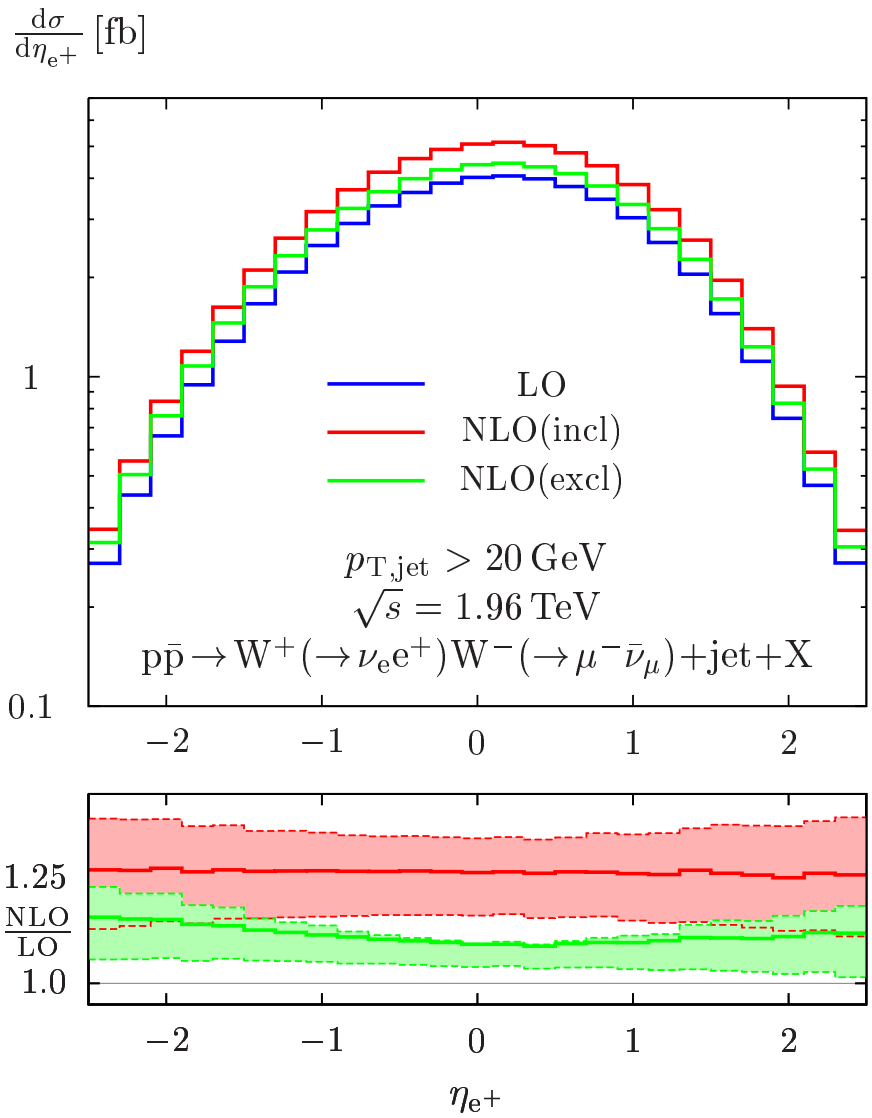

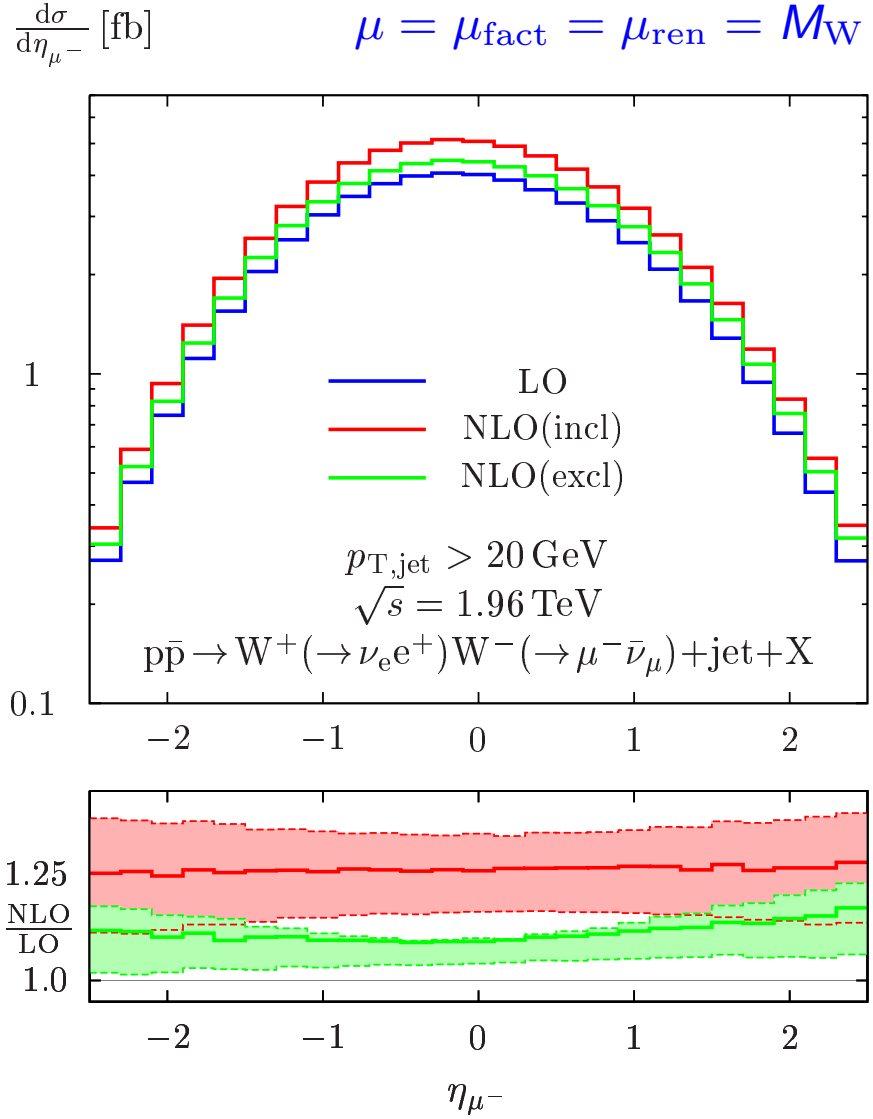

Jet rapidity, invariant mass of leptons at the Tevatron

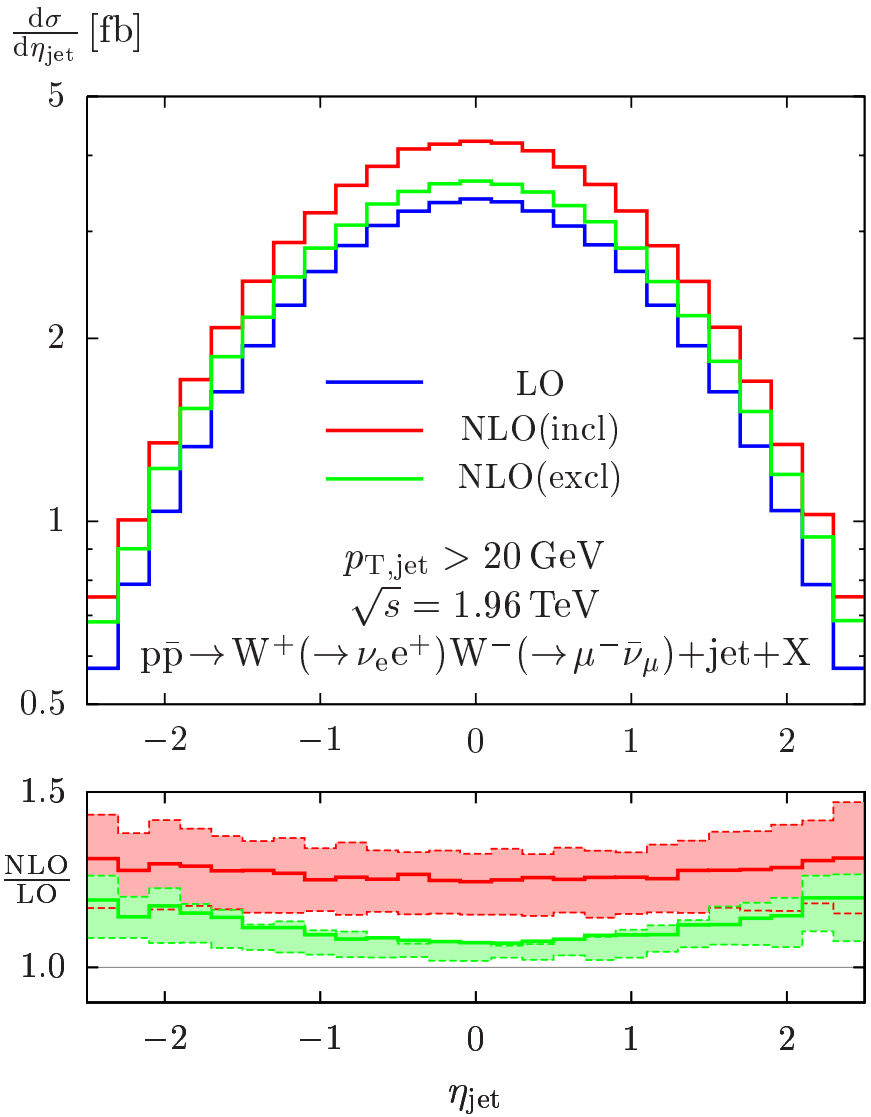

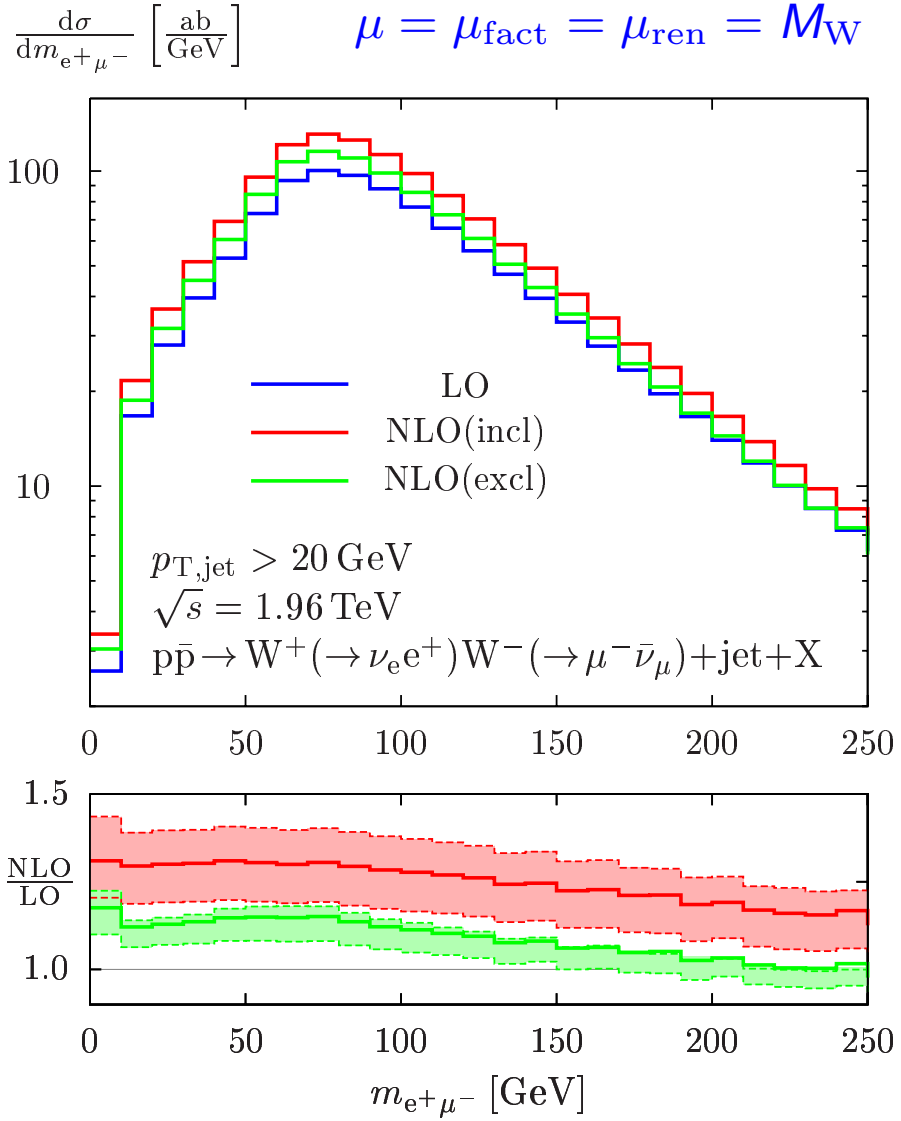

Collinear subtraction counterterm

- Real corrections: divergences resulting from collinear emission off incoming partons
  $\hookrightarrow$ no complete cancellation against virtual corrections
- Divergences are absorbed in redefined parton distribution functions (PDF's)

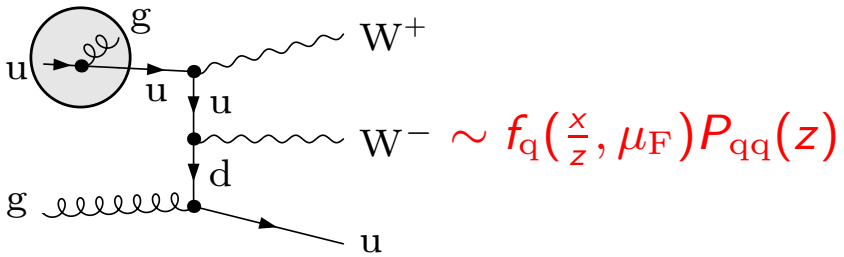

$\sim f_{\mathrm{q}}(\frac{x}{z},\mu_{\mathrm{F}})P_{\mathrm{qq}}(z)$

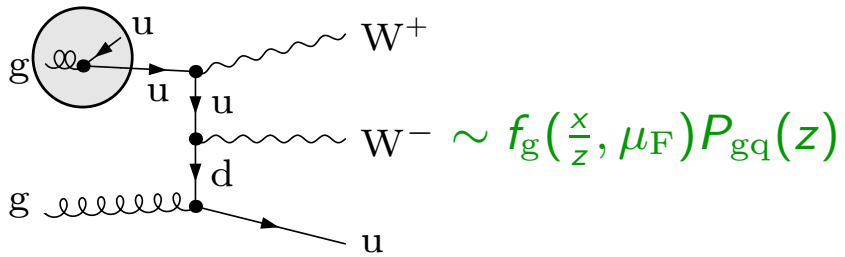

$\sim f_{\mathrm{g}}(\frac{x}{z},\mu_{\mathrm{F}})P_{\mathrm{gq}}(z)$

Corresponding redefinition of PDF's:

$P_{ij}(z)$ = Altarelli–Parisi splitting functions

$$
\begin{aligned}
f_{\mathrm{q}}(x,\mu_{\mathrm{F}}) \quad \to \quad & f_{\mathrm{q}}(x,\mu_{\mathrm{F}}) \\
& + \frac{\alpha_{\mathrm{s}}}{2\pi}\int_x^1 \frac{dz}{z} f_{\mathrm{q}}(\frac{x}{z},\mu_{\mathrm{F}}) \left(\frac{\Gamma(1+\varepsilon)}{\varepsilon}(4\pi)^{\varepsilon} + \ln\frac{\mu^2}{\mu_{\mathrm{F}}^2} \right) C_{\mathrm{F}}[P_{\mathrm{qq}}(z)]_+ \\
& + \frac{\alpha_{\mathrm{s}}}{2\pi}\int_x^1 \frac{dz}{z} f_{\mathrm{g}}(\frac{x}{z},\mu_{\mathrm{F}}) \left(\frac{\Gamma(1+\varepsilon)}{\varepsilon}(4\pi)^{\varepsilon} + \ln\frac{\mu^2}{\mu_{\mathrm{F}}^2} \right) T_{\mathrm{R}} P_{\mathrm{gq}}(z) \\
f_{\mathrm{g}}(x,\mu_{\mathrm{F}}) \quad \to \quad & \cdots \text{ analogously}
\end{aligned}
$$

Tuned comparison

Status of tuned comparison between results of [Dittmaier, S.K., Uwer '07], [Campbell, Ellis, Zanderighi '07] and [Binoth, Guillet, Karg, Kauer, Sanguinetti (in progress)]:

↪ [NLM Les Houches report '08]

- Integrated LO results checked:

$pp \to W^+W^-+jet+X$	σ_{LO}[fb]
DKU	10371.7(12)
CEZ	10372.26(97)
BGKKS	10371.7(11)

- Results for virtual corrections checked at one phase-space point:

$u\bar{u} \to W^+W^-g \qquad |\mathcal{M}_{LO}|^2/e^4 g_s^2 = 0.9963809154477200 \cdot 10^{-3}$

$$2\mathrm{Re}\{\mathcal{M}_V^* \cdot \mathcal{M}_{LO}\} = e^4 g_s^2 \Gamma(1+\varepsilon) \left(\frac{4\pi\mu^2}{M_W^2}\right)^{\varepsilon} \left(\frac{1}{\varepsilon^2} c_{-2} + \frac{1}{\varepsilon} c_{-1} + c_0\right)$$

All bosonic contributions:

$u\bar{u} \to W^+W^-g$	c_{-2}[GeV^{-2}]	c_{-1}^{bos}[GeV^{-2}]	c_0^{bos}[GeV^{-2}]
DKU	$-1.080699305508758 \cdot 10^{-4}$	$7.842861905263072 \cdot 10^{-4}$	$-3.382910915425372 \cdot 10^{-3}$
CEZ	$-1.080699305505865 \cdot 10^{-4}$	$7.842861905276719 \cdot 10^{-4}$	$-3.382910915464027 \cdot 10^{-3}$
BGKKS	$-1.080699305508814 \cdot 10^{-4}$	$7.842861905263293 \cdot 10^{-4}$	$-3.382910915616242 \cdot 10^{-3}$

Fermionic contributions for 2 light generations in the loop:

$u\bar{u} \to W^+W^-g$	$c_{-1}^{ferm1+2}$[GeV^{-2}]	$c_0^{ferm1+2}$[GeV^{-2}]
DKU	$2.542821895320379 \cdot 10^{-5}$	$4.372323372044527 \cdot 10^{-7}$
CEZ	$2.542821895311753 \cdot 10^{-5}$	$4.372790378087550 \cdot 10^{-7}$
BGKKS	$2.542821895314862 \cdot 10^{-5}$	$4.372324288356448 \cdot 10^{-7}$